INFLUENCE OF SHEAR DEFORMATIONS IN PLATE BENDING

by

Erdem Kaya

B.S., Civil Engineering, METU, 1996

M.S., Civil Engineering, Boğaziçi University, 1999

Submitted to the Institute for Graduate Studies in
Science and Engineering in partial fulfilment of
the requirements for the degree of
Doctor of Philosophy

Graduate Program in Civil Engineering

Boğaziçi University

2006

ACKNOWLEDGEMENTS

I would like to express my sincere thanks to my thesis supervisor, Prof. Dr. Semih S. Tezcan for his invaluable guidance, continuous support, and helpful suggestions. He has always been supportive for the preparation of this Thesis.

My sincere gratitude is also due to the members of my advisory committee Assoc. Prof. Dr. Osman Börekçi, Assoc. Prof. Dr. Gülten Gülay, Prof. Dr. Zeki Hasgür and Prof. Dr. Cengiz Karakoç, for their useful suggestions and comments.

Heartfelt thanks are due to my wife Şehnaz Bugay Kaya for her never ending help and understanding. I would also like to thank to my parents for their understanding and loving care. I would like to thank also Devrim Sönmez, Kenan Ertan, Nurçin Yenerer and Umut Sönmez, my schoolmates, for their encouragement and invaluable assistance during the preparation of the Thesis.

ABSTRACT

INFLUENCE OF SHEAR DEFORMATIONS IN PLATE BENDING

The influence of shear deformations in plate bending becomes significant when the ratio of the thickness to span is relatively large. However, the effects of transverse shear strains are neglected normally in classical theory and therefore, Kirchhoff thin plate theory is not adequate for providing accurate deflections, shear and bending moment values in both static and dynamic conditions. In order to include the influence of shear strains, the shear deformation theories, such as the first order shear deformation theory of Mindlin, is used.

Normally, for the analyses of relatively thick plates special category of solid finite elements incorporating the shear deformations are used. In this study, however, a new version of Hrennikoff lattice model has been introduced for the analysis of thick plates. The flexural stiffness properties of the individual members of the lattice model have been appropriately modified to take into account the influence of shear deformations. Thus, the complicated expressions and the extensive theoretical derivations involved in following the Mindlin's thick plate theory, are avoided. Further, the task of computer programming as well as the speed of computations have been simpler and much faster.

For purposes of illustration, a number of thick plates of square, rectangular and elliptical shapes and with different support conditions are analysed under the action of UDL and point load for varying thickness to span ratios. The results of analyses corresponding to a) the closed form solutions, b) the 2D and 3D solid finite elements, and c) the lattice model technique have been presented in a comparative fashion. It has been demonstrated that the newly introduced lattice model technique provides relatively very high degree of accuracy for thick plates, by using appropriate shape factors.

ÖZET

PLAKLARIN EĞİLMESİNDE KAYMA DEFORMASYONLARININ ETKİSİ

Plakların eğilme hesaplarında kayma deformasyonlarının etkisi, plağın kalınlık/açıklık oranlarının nispeten büyük olduğu durumlarda çok önemli bir rol oynamaktadır. Bununla birlikte, klasik teoride normal olarak kayma gerilmeleri ihmal edilmektedir. Dolayısı ile, Kirchhoff ince plak teorisi gittikçe kalınlaşan plaklarda statik ve dinamik sehimlerin kayma ve eğilme değerlerinin doğru değerlerini bulmakta yetersiz kalmaktadır. Bu nedenle, kayma gerilmelerini dahil edebilmek için Mindlin'in birinci derece kayma deformasyonları teorisi gibi kesin bir metot bu tezde temel dayanak olarak kullanılmıştır.

Normal olarak, kalın plakların çözümü için, literatürde kayma gerilmelerinin rolünü göz önüne alan iki boyutlu sonlu elemanlar mevcuttur. Ancak, bu çalışmada kalın plakların kesin çözümü için özel dikdörtgen Hrennikoff ızkara çubuk elemanları geliştirilmiştir. Kayma deformasyonlarının etkisi, ızkara çubuklarının eğilme rijitliklerine uygulanan bazı düzeltme faktörleri yardımı ile göz önüne alınmıştır. Böylece, Mindlin kalın plak teorisinin karmaşık formülasyonlarına dayanan sürekli sonlu elemanlara ihtiyaç kalmadığı gibi, bilgisayar programlama ve nümerik çözüm işlemleri de çök basitleştirilmiştir.

Önerilen metodun sağladığı avantajları ortaya çıkarabilmek amacı ile, kalınlığın açıklığa oranı gittikçe büyüyen kare, dikdörtgen ve elips şeklindeki plaklar uniform ve tekil yükler altında analiz edilmiştir. Analiz için ***a)*** ince plaklara ait kapalı çözüm formülleri, ***b)*** kalın plaklar için Mindlin teorisine göre geliştirilmiş sürekli sonlu elemanlar ve ***c)*** özel düzeltme faktörleri ile donatılmış ızkara modeli çubuk elemanlar kullanılmıştır.

Sonuçlar göstermiştir ki, bu tezde önerilen dikdörtgen ızkara çubuk elemanlar ve bunlara ait özel kayma düzeltme faktörleri kullanıldığı zaman, en kalın plaklar için bile, büyük bir hassasiyetle kesin çözüme yaklaşmak mümkün olmaktadır.

TABLE OF CONTENTS

LIST OF FIGURES

LIST OF TABLES

LIST OF SYMBOLS

{A}	Actions of the plate element
A_i, A_j	Stiffness coefficients
D	Flexural rigidity of the plate
{D}	Displacement and Rotations vector
E	Modulus of elasticity
F	Area of the cross-section
G	Shear modulus
I_d	Moment of inertia of diagonal element of the lattice cell
I_e	Moment of inertia of left and right element of the lattice cell
I_s	Moment of inertia of front and back element of the lattice cell
J_e	Torsional rigidity of left and right element of the lattice cell
J_s	Torsional rigidity of front and back element of the lattice cell
K_s	Shear correction factor in Mindlin Theory
k_s	Shape factor of unidimensional Hrennikoff bars
[K]	Total stiffness matrix
L	Length
M_{nn}, M_{ns}	Moments per unit length in normal and tangential coordinates (n,s)
M_{xx}, M_{yy}, M_{xy}	Moments per unit length
n_x, n_y	Direction cosines of the unit normal on the boundary
Q_x, Q_y	Shear forces
Q_n	Shear force in normal and tangential coordinates
q	Transverse load
t	Thickness of the plate
U	Strain energy
u	Displacement component along x-axis
V	Potential energy
v	Displacement component along y-axis
W	External work
w_0	Transverse deflection of a point on the mid-plane

α	Coefficient for plan dimension of plate
Γ	Boundary
γ	Shear correction factor
γ_{xy}	Shear strain
δU	Virtual strain energy
δV	Virtual potential energy
ε	Shear strain parameter, $\varepsilon = 1/(1+\gamma)$
$\varepsilon_{xx}, \varepsilon_{yy}$	Normal strains in x and y-directions
Θ	Rotational degree of freedom
λ_i, λ_{ij}	Shear correction factors
ν	Poisson ratio
σ_{xx}, σ_{yy}	Normal stresses in x and y-directions
σ_{xy}	Shear stress
ϕ_x	Rotation about y-axis
ϕ_y	Rotation about x-axis

1. INTRODUCTION

1.1. Influence of Shear Strains

The classical Kirchoff Plate Theory is not adequate in providing accurate shear and bending values both in static and dynamic conditions when the ratio of the thickness to side dimensions of the plate is relatively large. This is because the effects of transverse shear strains, which are neglected normally in the classical theory, become significant in relatively thick plates.

In order to include the influence of shear strains, the shear deformation theories, such as the first order shear deformation plate theory of Mindlin, may be successfully used in these conditions. The influence of shear deformations become pronounced as the thickness to side length ratio of the plate exceeds 1/10 and the effects of shear deformations increase parallel to the increase in this ratio.

As an alternate approach to incorporating the transverse shear strains, the Hrennikoff lattice model technique [1] may be used. A rectangular finite element is modelled by means of unidimensional lattice bars as originally introduced by A. Hrennikoff. A typical Hrennikoff lattice cell contains four unidimensional flexural bars rigidly connected to each other at the corners. They can carry torsional moments also. The two diagonal bars, however, can only transfer bending moments at their ends.

1.2. Conventional Methods in Plate Theory

The basic differential equation governing the deflection of thin plates was developed by Lagrange and Sophie Germain [2] in 1811 and was the first major contribution in the theory of thin plates to be presented.

Poisson [3], in a paper on elasticity published in 1829, set forth the investigation of the problem of an elastic plate using general equations of elasticity. Poisson's derivation

contains a set of boundary conditions; thus, he was able to obtain the solution for circular plates under symmetrical loading conditions.

Kirchhoff [4], in a paper published in 1850, derived the governing equation and the corresponding boundary conditions by using the energy principles or the principle of least work. In this paper, Kirchhoff was able to reduce by one the number of boundary conditions necessary to describe a free edge as proposed by Poisson.

1.3. Numerical Methods in Plate Theory

The analysis of elastic mediums by the use of a grid framework model was first presented in 1941 by A. Hrennikoff [1] in a paper which proposed a square grid model and utilized a constant Poisson's ratio of 1/3. Other writers such as Newmark [5], Ang and Newmark [6], and Yettram and Husain [7] have refined the technique by developing more general plane framework models. In addition, the special case of Poisson's ratio equal to zero was investigated by Christensen [8], Lightfoot [9], and Yettram and Husain [7].

As an alternate procedure to physical lattice models, the solid type mathematical models, called "finite elements" have been initially introduced by Turner, *et. al.* [10] and later have been extensively employed in continuum mechanics and also in other fields of engineering. The rectangular finite elements developed for the analysis of plate bending by Adini [11], Melosh [12, 13] , Clough, et. al. [14] and Zienkiewicz and Cheung [15] , are especially noteworthy.

It is certainly possible to utilise three dimensional finite elements, such as rectangular prisms, hexahedra, and tetrahedra, for the analysis of thick plate bending. Many examples of simple and complex shapes of three dimensional elements have been developed by Melosh [16], Argyris [17], and Fjeld [18].

The behaviour of thick plates has been investigated by several researchers. Reissner [19] derived expressions for moments and shear forces for isotropic elastic plates including the effects of shear deformation rotatory inertia, and vertical stress σ_z by using a variational principle. Later Mindlin [20] derived equations of motion for isotropic elastic plates

including the effects of shear deformation and rotatory inertia and obtained the equations to calculate stresses of a plate.

Triangular finite elements with and without curvature have been introduced by Utku [21], and quadrilateral elements by Clough and Felippa [22], for the analysis of thin and thick plate bending.

2. THIN PLATE (KIRCHHOFF) BENDING THEORY

2.1. General Definitions

A plate is a structural element whose lateral dimensions are large compared to its thickness and which is subjected to loads causing bending and stretching deformations. Because the thickness is in most cases no greater than one-tenth of the in-plane dimensions, it is often not necessary to model the plate by using 3-D elasticity equations.

The governing equations of plates can be derived by either using vector mechanics or energy principles. In vector mechanics, the forces and moments on an element are summed to obtain the equation of equilibrium or the motion. In energy methods, the principles of virtual work or their derivatives are used, such as the principles of minimum potential energy. Although both methods give same equations, the energy methods are advantageous in providing information on the form of the boundary conditions.

The two-dimensional plate theories can be classified into two categories:

1) Classical plate theory where the transverse shear deformations are neglected
2) Extended plate theory where the transverse shear deformations are considered.

Plate theories are developed by assuming the form of the displacement or stress field as linear combinations of unknown functions and the thickness coordinate. For the bending case, lines normal to the midsurface in the undeformed geometry remain normal to this surface in the deformed geometry. In other words, lines connecting the surfaces of the plate and normal to the xy plane in the undeformed geometry, translate vertically as rigid lines while maintaining the same coordinate values x and y. In addition, these lines rotate as rigid elements as a result of bending.

2.2. Assumptions of Thin Plate Theory

If the thickness of a plate is small compared to its span, i.e. smaller than one tenth of its span, a very satisfactory approximate theory of bending of the plate by lateral loads can be developed by making the following assumptions:

1. There remains no deformation in the middle plane of the plate. This plane remains neutral during bending
2. Points of the plate lying initially on a normal-to-the-middle plane of the remain on the normal-to-the-middle surface of the plate after bending
3. The normal stresses in the direction transverse to the plate can be disregarded.

Using these assumptions, all stress components can be expressed by deflection, *w,* of the plate, which is a function of the two coordinates in the plane of the plate. This function has to satisfy a linear partial differential equation, which, together with the boundary conditions, completely defines *w*. Thus the solution of this equation gives all necessary information for calculating stresses at any point of the plate [23].

2.3. Displacements and Strains

The Kirchhoff plate theory for the pure bending case is based on the displacement field:

$$u(x, y, z) = -z\frac{\partial w_0}{\partial x} \tag{2.1a}$$

$$v(x, y, z) = -z\frac{\partial w_0}{\partial y} \tag{2.1b}$$

$$w(x, y, z) = w_0(x, y) \tag{2.1c}$$

where u,v and w are displacement components along the x,y and z coordinate directions respectively and w_0 is the transverse shear deflections of a point on the mid-plane (i.e. z=0). The Kirchhoff assumption neglects both transverse shear and transverse normal effects, it is to say that deformation is entirely due to bending and in-plane stretching [24].

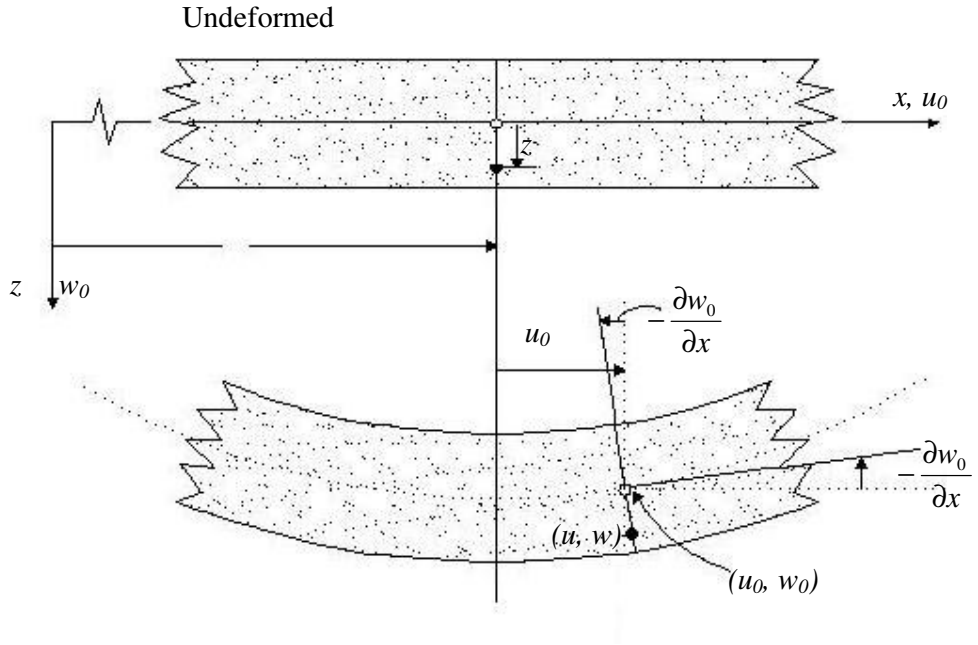

Figure 2.1. Undeformed and deformed geometries of an edge of a plate

The principle of virtual displacements has been used in the derivation of the equilibrium equations and the boundary conditions. The non-zero linear strains associated with the displacement field in Equations (2.1.a-c) are

$$\varepsilon_{xx} = \frac{\partial u}{\partial x} = -z\frac{\partial^2 w_0}{\partial x^2} \tag{2.2a}$$

$$\varepsilon_{yy} = \frac{\partial v}{\partial y} = -z\frac{\partial^2 w_0}{\partial y^2} \tag{2.2b}$$

$$\gamma_{xy} = \frac{\partial u}{\partial y} + \frac{\partial v}{\partial x} = -2z\frac{\partial^2 w_0}{\partial x \partial y} \tag{2.2c}$$

Q_y

M_{yy} N_{yy}

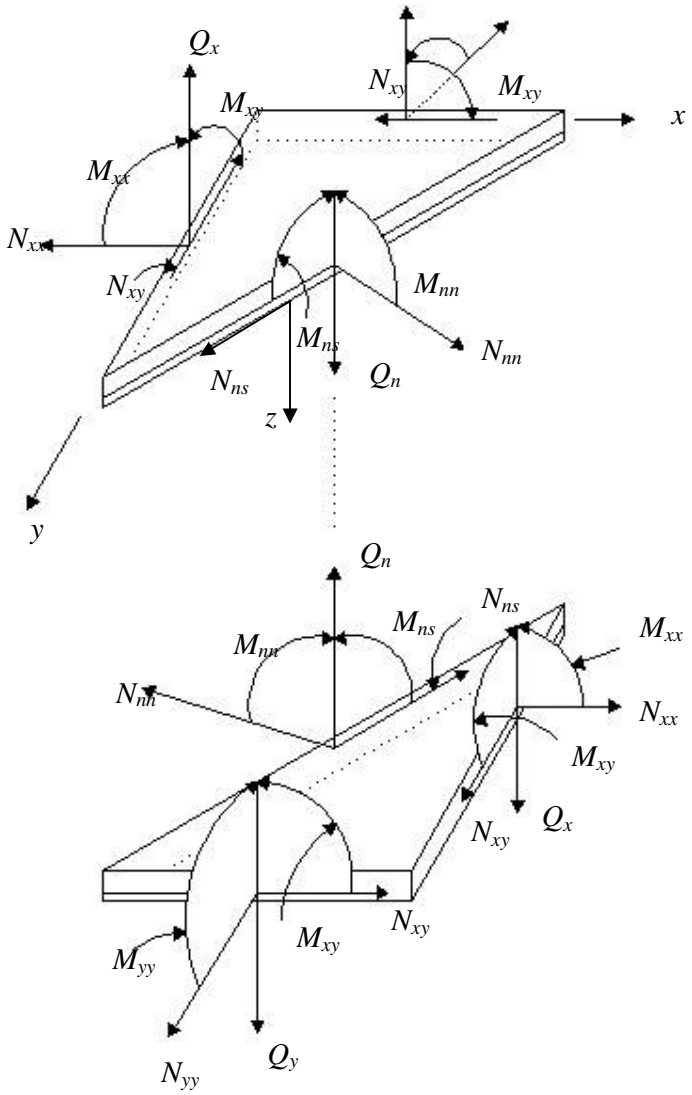

Figure 2.2. Forces and moments on a plate element

where ε_{xx} and ε_{yy} are normal strains and γ_{xy} is the shear strain ($\gamma_{xz} = \gamma_{yz} = 0$ in the Kirchhoff plate theory) .

2.4. Principle of Virtual Work and Equations of Equilibrium

The virtual strain energy U of the Kirchhoff plate theory is given by

$$\delta U = \int_{\Omega_0} \left[\int_{-\frac{h}{2}}^{\frac{h}{2}} \left(\sigma_{xx} \delta\varepsilon_{xx} + \sigma_{yy} \delta\varepsilon_{yy} + \sigma_{xy} \delta\gamma_{xy} \right) dz \right] dxdy$$

$$= -\int_{\Omega_0} \left(M_{xx} \frac{\partial^2 \delta w_0}{\partial x^2} + M_{yy} \frac{\partial^2 \delta w_0}{\partial y^2} + 2M_{xy} \frac{\partial^2 \delta w_0}{\partial x \partial y} \right) dxdy \tag{2.3}$$

where Ω_0 denotes the domain corresponding to the mid-plane of the plate, t being the thickness of the plate, M_{xx}, M_{yy} and M_{xy} the moments per unit length.

$$\begin{Bmatrix} M_{xx} \\ M_{yy} \\ M_{xy} \end{Bmatrix} = \int_{-\frac{t}{2}}^{\frac{t}{2}} \begin{Bmatrix} \sigma_{xx} \\ \sigma_{yy} \\ \sigma_{xy} \end{Bmatrix} z \, dz \tag{2.4}$$

The virtual potential energy δV due to transverse load $q(x,y)$ is

$$\delta W = -\int_{\Omega_0} q(x, y) \, \delta w_0 \, dxdy \tag{2.5}$$

The principle of virtual displacements requires that $\delta P = \delta U + \delta W = 0$. Using divergence theorem, the following is obtained;

$$\begin{aligned} 0 &= -\int_{\Omega_0} \left(M_{xx} \frac{\partial^2 \delta w_0}{\partial x^2} + M_{yy} \frac{\partial^2 \delta w_0}{\partial y^2} + 2M_{xy} \frac{\partial^2 \delta w_0}{\partial x \partial y} + q \, \delta w_0 \right) dxdy \\ &= -\int_{\Omega_0} \left(M_{xx,xx} + 2M_{xy,xy} + M_{yy,yy} + q \right) \delta w_0 \, dxdy \\ &\quad - \oint_{\Gamma} \left[\left(M_{xx} n_x + M_{xy} n_y \right) \frac{\partial \delta w_0}{\partial x} + \left(M_{xy} n_x + M_{yy} n_y \right) \frac{\partial \delta w_0}{\partial y} \right] ds \\ &\quad + \oint_{\Gamma} \left[\left(M_{xx,x} + M_{xy,y} \right) n_x + \left(M_{xy,x} + M_{yy,y} \right) n_y \right] \delta w_0 ds \end{aligned} \tag{2.6}$$

where a comma followed by subscripts denotes differentiation with respect to the subscripts, i.e., $M_{xx,x} = \partial M_{xx} / \partial dx$, n_x and n_y denote the direction cosines of the unit normal $\hat{n}$ on the boundary Γ, and a circle on the integral sign signifies integration over the total boundary. Also s is the coordinate measured along Γ. If the unit normal vector is oriented at an angle θ from the positive x-axis, then $n_x = Cos\theta$ and $n_y = Sin\theta$. Since δw_0 is arbitrary in Ω_0, and it is independent of $\partial \delta w_0 / \partial x$ and $\partial \delta w_0 / \partial y$ on the boundary Γ, it follows that

$$\frac{\partial^2 M_{xx}}{\partial x^2} + 2\frac{\partial^2 M_{xy}}{\partial x \partial y} + \frac{\partial^2 M_{yy}}{\partial y^2} + q = 0 \quad \text{in } \Omega_0 \tag{2.7}$$

forming the equilibrium equation of the Kirchhoff plate theory.

2.5. Boundary Conditions

For the determination of the boundary conditions, boundary integrals in Equation 2.6 will be used. On an edge parallel to x or y-axis, the boundary expression shows that

$$\text{either} \quad \delta w_0 = 0 \quad \text{or} \quad Q_x n_x + Q_y n_y = 0 \tag{2.8a}$$

$$\text{either} \quad \frac{\partial \delta w_0}{\partial x} = 0 \quad \text{or} \quad M_{xx} n_x + M_{xy} n_y = 0 \tag{2.8b}$$

$$\text{either} \quad \frac{\partial \delta w_0}{\partial y} = 0 \quad \text{or} \quad M_{xy} n_x + M_{yy} n_y = 0 \tag{2.8c}$$

where

$$Q_x \equiv M_{xx,x} + M_{xy,y} \ , \quad Q_y \equiv M_{yy,y} + M_{xy,x} \tag{2.9}$$

Equations (2.8a-c) indicate that $w_0, \frac{\partial w_0}{\partial x}$ and $\frac{\partial w_0}{\partial y}$ are the primary variables. The associated secondary variables are $Q_x n_x + Q_y n_y$, $M_{xx} n_x + M_{xy} n_y$ and $M_{xy} n_x + M_{yy} n_y$. The specification of any primary variable constitutes as essential (or geometric) boundary condition, and any secondary variable constitutes a natural (or force) boundary condition.

It is useful to express the slopes and moments in terms of normal and tangential coordinates since not every edge of the plate is parallel to a coordinate axis.

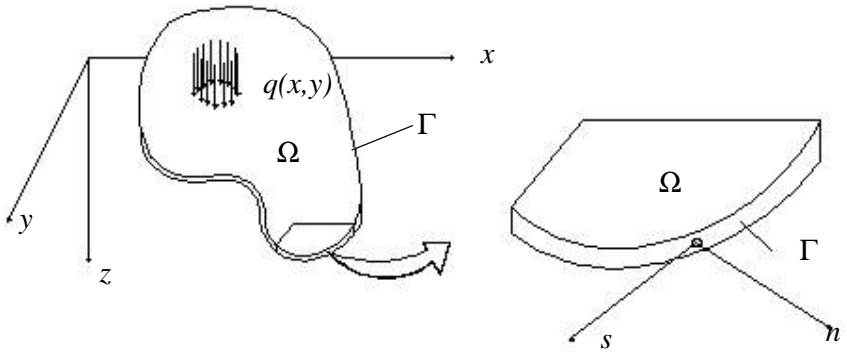

Figure 2.3. Plate element with a curved boundary and coordinate system (n,s,z)

$$\frac{\partial w_0}{\partial x} = n_x \frac{\partial w_0}{\partial n} - n_y \frac{\partial w_0}{\partial s} \tag{2.10a}$$

$$\frac{\partial w_0}{\partial y} = n_y \frac{\partial w_0}{\partial n} + n_x \frac{\partial w_0}{\partial s} \tag{2.10b}$$

and the boundary expression in *Equation 2.6* can be expressed in terms of normal and tangential derivatives of w_0

$$\oint_\Gamma \left[\left(Q_x n_x + Q_y n_y\right)\delta w_0 - \left(M_{xx} n_x + M_{xy} n_y\right)\left(\frac{\partial \delta w_0}{\partial n} n_x - \frac{\partial \delta w_0}{\partial s} n_y \right) \right.$$
$$\left. - \left(M_{xy} n_x + M_{yy} n_y\right)\left(\frac{\partial \delta w_0}{\partial n} n_y + \frac{\partial \delta w_0}{\partial s} n_x \right) \right] ds$$

$$= \oint_\Gamma \left[\left(Q_x n_x + Q_y n_y\right)\delta w_0 - \left(M_{xx} n_x^2 + 2M_{xy} n_x n_y + M_{yy} n_y^2\right) \frac{\partial \delta w_0}{\partial n} \right.$$
$$\left. - \left[\left(M_{yy} - M_{xx}\right) n_x n_y + M_{xy}\left(n_x^2 - {}_y^2\right) \right] \frac{\partial \delta w_0}{\partial s} \right] ds \tag{2.11}$$

primary variables: $w_0, \frac{\partial w_0}{\partial n}, \frac{\partial w_0}{\partial s}$ (2.12a)

secondary variables: Q_n, M_{nn}, M_{ns} (2.12b)

where

$$Q_n \equiv Q_x n_x + Q_y n_y \tag{2.13a}$$

$$M_{nn} \equiv M_{xx} n_x^2 + 2M_{xy} n_x n_y + M_{yy} n_y^2 \tag{2.13b}$$

$$M_{ns} \equiv \left(M_{yy} - M_{xx}\right) n_x n_y + M_{xy}\left(n_x^2 - {}_y^2\right) \tag{2.13c}$$

Supposing that the material of the plate is isotropic and obeys Hooke's Law, then the stress strain relations are given by:

$$\begin{Bmatrix} \sigma_{xx} \\ \sigma_{yy} \\ \sigma_{xy} \end{Bmatrix} = \frac{E}{1-\nu^2} \begin{bmatrix} 1 & \nu & 0 \\ \nu & 1 & 0 \\ 0 & 0 & \frac{(1-\nu)}{2} \end{bmatrix} \begin{Bmatrix} \varepsilon_{xx} \\ \varepsilon_{yy} \\ \gamma_{xy} \end{Bmatrix} \tag{2.14}$$

$$M_{xx} = \int_{-\frac{t}{2}}^{\frac{t}{2}} \sigma_{xx} z\, dz = \frac{E}{\left(1-\nu^2\right)} \int_{-\frac{t}{2}}^{\frac{t}{2}} \left(\varepsilon_{xx} + \nu\varepsilon_{yy}\right) z dz = -D\left(\frac{\partial^2 w_0}{\partial x^2} + \nu \frac{\partial^2 w_0}{\partial y^2} \right) \tag{2.15a}$$

$$M_{yy} = \int_{-\frac{t}{2}}^{\frac{t}{2}} \sigma_{yy} z\, dz = \frac{E}{\left(1-\nu^2\right)} \int_{-\frac{t}{2}}^{\frac{t}{2}} \left(\varepsilon_{yy} + \nu\varepsilon_{xx}\right) z dz = -D\left(\nu \frac{\partial^2 w_0}{\partial x^2} + \frac{\partial^2 w_0}{\partial y^2} \right) \tag{2.15b}$$

$$M_{xy} = \int_{-\frac{t}{2}}^{\frac{t}{2}} \sigma_{xy} z\, dz = G \int_{-\frac{t}{2}}^{\frac{t}{2}} \gamma_{xy}\, z dz = -(1-\nu) D \frac{\partial^2 w_0}{\partial x \partial y} \tag{2.15c}$$

where

$$D = \frac{Eh^3}{12\left(1-\nu^2\right)} \tag{2.16}$$

Substituting the expressions into *Equation 2.7*, the biharmonic equation is obtained.

$$D\left(\frac{\partial^4 w_0}{\partial x^4} + 2 \frac{\partial^4 w_0}{\partial x^2 \partial y^2} + \frac{\partial^4 w_0}{\partial y^4} \right) = q \tag{2.17}$$

$$D\nabla^2 \nabla^2 w_0 = q \quad \text{or} \quad D\nabla^4 w_0 = q \tag{2.18}$$

Correct boundary conditions for the Kirchhoff plate theory are

Generalized displacements $w_0, \ \frac{\partial w_0}{\partial n}$ (2.19)

Generalized forces $V_n, \ M_{nn}$ (2.20)

Thus, the boundary conditions involve specifying these variables. The edge conditions for the Kirchhoff plate theory are

a) Free Edge

$$w_0 \neq 0, \ \frac{\partial w_0}{\partial y} \neq 0, \tag{2.21}$$

but the edge may have applied forces and moments

$$V_y = \hat{V}_y, \ M_{yy} = \hat{M}_{yy} \tag{2.22}$$

b) Simply Supported Edge

$$w_0 = 0, \ M_{yy} = \hat{M}_{yy} \tag{2.23}$$

c) Fixed (clamped) Edge

$$w_0 = 0, \ \frac{\partial w_0}{\partial y} = 0 \tag{2.24}$$

3. THICK PLATE (MINDLIN) THEORY

3.1 Displacements and Strains

The approximate theories of thin plates, become unreliable in the case of plates of considerable thickness, especially in the case of highly concentrated loads. In such a case the thick-plate theory should be applied. There are a number of shear deformation plate theories. The simplest is the first order shear deformation plate theory or Mindlin plate theory and based on the displacement field;

$$u(x, y, z) = z\phi_x(x, y) \tag{3.1a}$$

$$v(x, y, z) = z\phi_y(x, y) \tag{3.1b}$$

$$w(x, y, z) = w_0(x, y) \tag{3.1c}$$

where ϕ_x and $-\phi_y$ are rotations about x and y-axes. The Mindlin plate theory extends the kinematics of the classical theory by introducing the transverse shear term, which is assumed to be constant on the thickness coordinate. The shear correction factors are needed to correct the computed shear deformations with respect to the actual shear force distributions. These shear correction factors depend not only on the geometric parameters but also on the loading and boundary conditions [24]. The linear strain components become

$$\varepsilon_{xx} = z\frac{\partial\phi_x}{\partial x} \tag{3.2a}$$

$$\varepsilon_{yy} = z\frac{\partial\phi_y}{\partial y} \tag{3.2b}$$

$$\gamma_{xy} = z\left(\frac{\partial\phi_x}{\partial y} + \frac{\partial\phi_y}{\partial x}\right) \tag{3.2c}$$

$$\gamma_{xz} = \phi_x + \frac{\partial w_0}{\partial x} \tag{3.2d}$$

$$\gamma_{yz} = \phi_y + \frac{\partial w_0}{\partial y} \tag{3.2e}$$

the shear strains ε_{xx}, ε_{yy} and γ_{xy} are linear through the plate thickness, while the transverse shear strains are γ_{xz} and γ_{yz} constant.

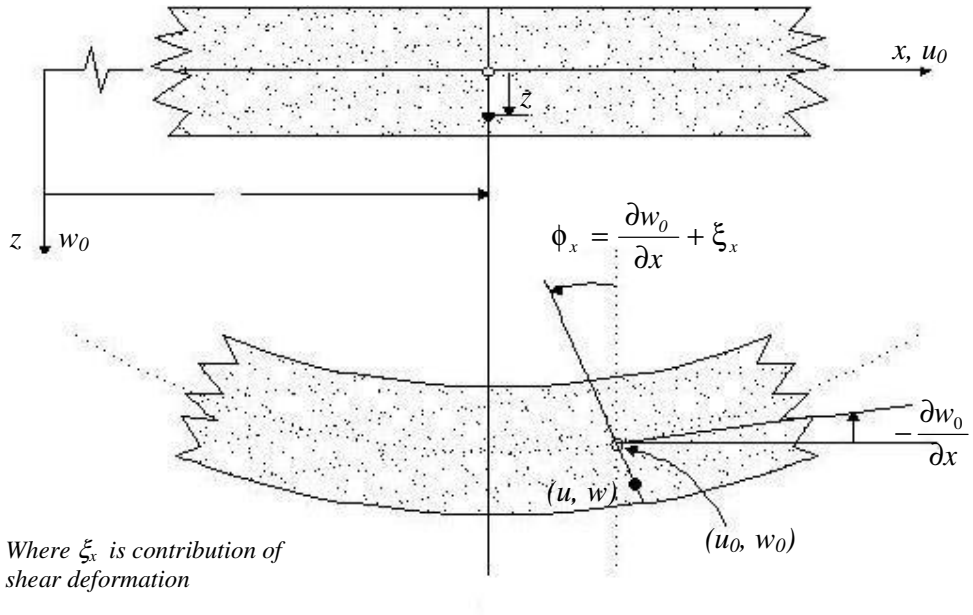

Figure 3.1. Undeformed and deformed geometries of an edge of a Mindlin plate

3.2. Equations of Equilibrium

The equations of equilibrium are derived using the principle of virtual displacements.

$$\delta P = \delta U + \delta W = 0 \tag{3.3a}$$

$$\delta U = \int_{\Omega_0} \left[\int_{-\frac{t}{2}}^{\frac{t}{2}} \left(\sigma_{xx}\delta\varepsilon_{xx} + \sigma_{yy}\delta\varepsilon_{yy} + \sigma_{xy}\delta\gamma_{xy} + \sigma_{xz}\delta\gamma_{xz} + \sigma_{yz}\delta\gamma_{yz} \right) dz \right] dxdy \tag{3.3b}$$

$$\delta W = -\int_{\Omega_0} q(x, y)\delta w_0 dxdy \tag{3.3c}$$

Substituting and integrating through the thickness of the plate,

$$0 = \int_{\Omega_0} \left[M_{xx} \frac{\partial \delta\phi_x}{\partial x} + M_{yy} \frac{\partial \delta\phi_y}{\partial y} + M_{xy} \left(\frac{\partial \delta\phi_x}{\partial y} + \frac{\partial \delta\phi_y}{\partial x} \right) - q\delta w_0 + Q_x \left(\frac{\partial \delta w_0}{\partial x} + \delta\phi_x \right) \right.$$

$$\left. + Q_y \left(\frac{\partial \delta w_0}{\partial y} + \delta\phi_y \right) \right] dxdy \tag{3.4}$$

The transverse shear stresses will be constant through the thickness like the shear strains. However, this is contradicting the fact that the transverse shear stresses are parabolic through the plate thickness. This variation can be corrected by introducing a parameter K_s called the shear correction factor.

$$\begin{Bmatrix} Q_x \\ Q_y \end{Bmatrix} = K_s \int_{-\frac{t}{2}}^{\frac{t}{2}} \begin{Bmatrix} \sigma_{xz} \\ \sigma_{yz} \end{Bmatrix} dz \tag{3.5}$$

K_s is found by equating the strain energy due to the transverse shear stresses of the Mindlin Theory with the strain energy due to transverse shear stresses of the three-dimensional elasticity theory. Integrating by parts Equation 3.4 and using divergence theorem;

$$0 = \int_{\Omega_0} \left[-\left(M_{xx,x} + M_{xy,y} - Q_x \right) \delta\phi_x - \left(M_{xy,x} + M_{yy,y} - Q_y \right) \delta\phi_y - \left(Q_{x,y} + Q_{y,y} + q \right) \delta w_0 \right] dxdy$$
$$+ \oint_{\Gamma} \left(Q_n \delta w_0 + M_{nn} \delta\phi_n + M_{ns} \delta\phi_s \right) ds \tag{3.6}$$

where $\phi_x = n_x\phi_n - n_y\phi_s$ and $\phi_y = n_y\phi_n + n_x\phi_s$ The equilibrium equations are

$$\delta w_0: \qquad -\left(\frac{\partial Q_x}{\partial x} + \frac{\partial Q_y}{\partial y} \right) = q \tag{3.7a}$$

$$\delta\phi_x: \qquad -\left(\frac{\partial M_{xx}}{\partial x} + \frac{\partial M_{xy}}{\partial y} \right) + Q_x = 0 \tag{3.7b}$$

$$\delta\phi_y: \quad -\left(\frac{\partial M_{yy}}{\partial y} + \frac{\partial M_{xy}}{\partial x} \right) + Q_y = 0 \tag{3.7c}$$

Primary variables: w_0, ϕ_n, ϕ_s (3.8a)

Secondary variables: Q_n, M_{nn}, M_{ns} (3.8b)

where

$$Q_n \equiv Q_x n_x + Q_y n_y \tag{3.9}$$

Supposing that the material of the plate is isotropic and obeys Hooke's Law, then the stress strain relations are given by:

$$\begin{Bmatrix} \sigma_{xx} \\ \sigma_{yy} \\ \sigma_{xy} \\ \sigma_{xz} \\ \sigma_{yz} \end{Bmatrix} = \frac{E}{1-\nu^2} \begin{bmatrix} 1 & \nu & 0 & 0 & 0 \\ \nu & 1 & 0 & 0 & 0 \\ 0 & 0 & \frac{(1-\nu)}{2} & 0 & 0 \\ 0 & 0 & 0 & \frac{(1-\nu)}{2} & 0 \\ 0 & 0 & 0 & 0 & \frac{(1-\nu)}{2} \end{bmatrix} \begin{Bmatrix} \varepsilon_{xx} \\ \varepsilon_{yy} \\ \gamma_{xy} \\ \gamma_{xz} \\ \gamma_{yz} \end{Bmatrix} \tag{3.10}$$

$$M_{xx} = \int_{-\frac{t}{2}}^{\frac{t}{2}} \sigma_{xx} z\, dz = \frac{E}{(1-\nu^2)} \int_{-\frac{t}{2}}^{\frac{t}{2}} (\varepsilon_{xx} + \nu\varepsilon_{yy}) z dz = D\left(\frac{\partial \phi_x}{\partial x} + \nu \frac{\partial \phi_y}{\partial y} \right) \tag{3.11a}$$

$$M_{yy} = \int_{-\frac{t}{2}}^{\frac{t}{2}} \sigma_{yy} z\, dz = \frac{E}{(1-\nu^2)} \int_{-\frac{t}{2}}^{\frac{t}{2}} (\varepsilon_{yy} + \nu\varepsilon_{xx}) z dz = D\left(\nu \frac{\partial \phi_x}{\partial x} + \frac{\partial \phi_y}{\partial y} \right) \tag{3.11b}$$

$$M_{xy} = \int_{-\frac{t}{2}}^{\frac{t}{2}} \sigma_{xy} z\, dz = G\int_{-\frac{t}{2}}^{\frac{t}{2}} \gamma_{xy}\, z dz = \frac{(1-\nu)D}{2} \left(\frac{\partial \phi_x}{\partial y} + \frac{\partial \phi_y}{\partial x} \right) \tag{3.11c}$$

$$Q_x = K_s \int_{-\frac{t}{2}}^{\frac{t}{2}} \sigma_{xx}\, dz = G\int_{-\frac{t}{2}}^{\frac{t}{2}} \gamma_{xz}\, dz = \frac{K_s E t}{2(1+\nu)} \left(\phi_x + \frac{\partial w_o}{\partial x} \right) \tag{3.11d}$$

$$Q_y = K_s \int_{-\frac{t}{2}}^{\frac{t}{2}} \sigma_{yy}\, dz = G\int_{-\frac{t}{2}}^{\frac{t}{2}} \gamma_{yz}\, dz = \frac{K_s E t}{2(1+\nu)} \left(\phi_y + \frac{\partial w_o}{\partial y} \right) \tag{3.11e}$$

By substituting force and moment resultants into *Equation 3.7*:

$$-\frac{K_s E t}{2(1+\nu)} \left(\frac{\partial^2 w_0}{\partial x^2} + \frac{\partial^2 w_0}{\partial y^2} + \frac{\partial \phi_x}{\partial x} + \frac{\partial \phi_y}{\partial y} \right) = q(x, y) \tag{3.12a}$$

$$-\frac{D(1-\nu)}{2}\left(\frac{\partial^2\phi_x}{\partial x^2}+\frac{\partial^2\phi_x}{\partial y^2}\right)-\frac{D(1+\nu)}{2}\frac{\partial}{\partial x}\left(\frac{\partial\phi_x}{\partial x}+\frac{\partial\phi_y}{\partial y}\right)+\frac{K_sEt}{2(1+\nu)}\left(\frac{\partial w_0}{\partial x}+\phi_x\right)=0$$

$$-\frac{D(1-\nu)}{2}\left(\frac{\partial^2\phi_y}{\partial y^2}+\frac{\partial^2\phi_y}{\partial x^2}\right)-\frac{D(1+\nu)}{2}\frac{\partial}{\partial x}\left(\frac{\partial\phi_x}{\partial x}+\frac{\partial\phi_y}{\partial y}\right)+\frac{K_sEt}{2(1+\nu)}\left(\frac{\partial w_0}{\partial y}+\phi_y\right)=0$$

by introducing the moment sum M and using Laplace operator

$$M \equiv \frac{M_{xx}+M_{yy}}{1+\nu}=D\left(\frac{\partial\phi_x}{\partial x}+\frac{\partial\phi_y}{\partial y}\right) \tag{3.13}$$

$$-\frac{K_sEt}{2(1+\nu)}\left(\nabla^2 w_0+\frac{M}{D}\right)=q(x,y) \tag{3.14a}$$

$$-D(1-\nu)\nabla^2\phi_x-(1+\nu)\frac{\partial M}{\partial x}+\frac{K_sEt}{(1+\nu)}\left(\frac{\partial w_0}{\partial x}+\phi_x\right)=0 \tag{3.14b}$$

$$-D(1-\nu)\nabla^2\phi_y-(1+\nu)\frac{\partial M}{\partial y}+\frac{K_sEt}{(1+\nu)}\left(\frac{\partial w_0}{\partial y}+\phi_y\right)=0 \tag{3.15c}$$

$$Q_n = K_sGt\left(\phi_n+\frac{\partial w_0}{\partial n}\right) \tag{3.16a}$$

$$M_{nn} = D\left(\frac{\partial\phi_n}{\partial n}+\frac{\partial\phi_s}{\partial s}\right) \tag{3.16b}$$

$$M_{ns} = \frac{D(1-\nu)}{2}\left(\frac{\partial\phi_n}{\partial s}+\frac{\partial\phi_s}{\partial n}\right) \tag{3.16c}$$

3.3. Boundary Conditions

The edge conditions for the Mindlin plate theory are

a) Free Edge

$$Q_n = 0,\ M_{nn} = 0,\ \ M_{ns} = 0$$

b) Simply Supported Edge (Hard type)

$$w_0 = 0, \quad M_{nn} = 0, \quad \phi_s = 0 \tag{3.18}$$

c) Simply Supported Edge (Soft type)

$$w_0 = 0, \quad M_{nn} = 0, \quad M_{ns} = 0 \tag{3.19}$$

d) Fixed (clamped) Edge

$$w_0 = 0, \quad \phi_n = 0, \quad \phi_s = 0 \tag{3.20}$$

3.4. Shear Correction Factors

Mindlin [20] pointed out that for an isotropic plate, the shear correction factor K_s depends on Poisson's ratio ν and it may vary from $K_s = 0.76$ for $\nu = 0$ to $K_s = 0.91$ for $\nu = 0.5$. Following Mindlin's suggestion of equating the angular frequency of the first antisymmetric mode of thickness-shear vibration according to the exact three-dimensional theory to the corresponding frequency according to his theory, it can be shown that the shear correction factor is given by the following cubic equation:

$$(K_s)^3 - 8(K_s)^2 + \frac{8(2-\nu)K_s}{1-\nu} - \frac{8}{1-\nu} = 0 \tag{3.21}$$

For example, if $\nu = 0.3$, then $K_s = 0.86$ and if $\nu = 0.176$, then $K_s = \pi^2/12$.

On the other hand, comparing the Mindlin plate equations for the constitutive shear forces with the ones proposed by Reissner [25], who assumed a parabolic variation of the shear stress distribution, the implicit shear correction factor of Reissner takes the value of

$$K_s = \frac{5}{6} \tag{3.22}$$

Based on an analytical vibration solution of three-dimensional, simply supported, rectangular, isotropic plate, Wittrick [26] performed a calibration of the Mindlin shear correction factor. He proposed that the shear correction factor be given by

$$K_s = \frac{5}{6 - \nu} \tag{3.23}$$

Wittrick's shear correction factor gives a value of 0.877 for $\nu = 0.3$, which corresponds closely to the value of 0.88. It appears that the Wittrick shear correction factor is the best to date as it has a simple form and allows for the effect of Poisson's ratio.

On the other hand, from the comparison of the Kirchhoff plate theory and the Mindlin plate theory Wang et al. [24] determined that the value of the shear correction factor K_s, varies between $K_s = 14/17$ and $K_s = 5/6$.

4. SOLUTION OF THIN PLATES BY FINITE ELEMENTS

4.1. Element Type

The 12-degrees-of-freedom flat-plate bending element, which will be considered for the finite element analysis, is shown in Figure 4.1. Each node has 3 degrees of freedom - a transverse displacement *w* in the *z* direction, a rotation θ_x about the *x* axis, and a rotation θ_y about the *y* axis.

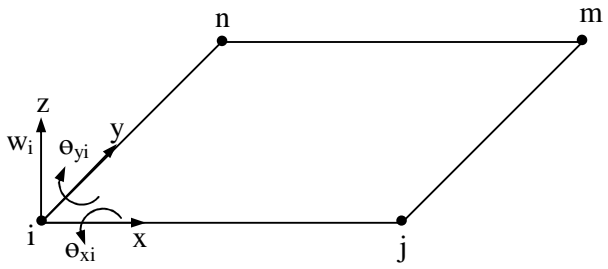

Figure 4.1. Typical plate bending finite element

The nodal displacement matrix at node *i* is given by

$$\{d_i\} = \begin{Bmatrix} w_i \\ \theta_{xi} \\ \theta_{yi} \end{Bmatrix} \tag{4.1}$$

where the rotations are related to the transverse displacement by

$$\theta_x = +\frac{\partial w}{\partial y} \quad \text{and} \quad \theta_y = -\frac{\partial w}{\partial x} \tag{4.2}$$

The negative sign on θ_y is due to the fact that a negative displacement *w* is required to produce a positive rotation to the *y* axis.

The total element displacement matrix is now given by

$$\{d\} = \{\underline{d}_i \quad \underline{d}_j \quad \underline{d}_m \quad \underline{d}_n\}^T \tag{4.3}$$

4.2. The Displacement Function

Because there are 12 total degrees of freedom for the element, we select a 12-term polynominal in x and y as follows:

$$w = a_1 + a_2 x + a_3 y + a_4 x^2 + a_5 xy + a_6 y^2 + a_7 x^3 + a_8 x^2 y + a_9 xy^2 + a_{10} y^3 + a_{11} x^3 y + a_{12} xy^3 \tag{4.4}$$

The constant a_1 through a_{12} can b e determined by expressing the 12 simultaneous equations linking the values of w and its slopes at the nodes when the coordinates take up their appropriate values [27]. First, we write

$$\begin{Bmatrix} w \\ +\dfrac{\partial w}{\partial y} \\ -\dfrac{\partial w}{\partial x} \end{Bmatrix} = \begin{bmatrix} 1 & x & y & x^2 & xy & y^2 & x^3 & x^2 y & xy^2 & y^3 & x^3 y & xy^3 \\ 0 & 0 & +1 & 0 & +x & +2y & 0 & +x^2 & +2xy & +3y^2 & +x^3 & +3xy^2 \\ 0 & -1 & 0 & -2x & -y & 0 & -3x^2 & -2xy & -y^2 & 0 & -3x^2 y & -y^3 \end{bmatrix} x \begin{Bmatrix} a_1 \\ a_2 \\ a_3 \\ \vdots \\ a_{12} \end{Bmatrix} \tag{4.5}$$

or in simple matrix form the degrees of freedom matrix is

$$\{\psi\} = [P]\{a\} \tag{4.6}$$

where $[P]$ is the 3×12 first matrix on the right side of Equation (4.5).

Next Equation (4.5) is evaluated at each node point as follows

$$\{d\} = \begin{Bmatrix} w_i \\ \theta_{xi} \\ \theta_{yi} \\ w_j \\ \vdots \end{Bmatrix} \begin{bmatrix} 1 & x_i & y_i & x_i^2 & x_i y_i & y_1^2 & x_i^3 & x_i^2 y_i & x_i y_i^3 & y_i^3 & x_i^3 y_i & x_i y_i^3 \\ 0 & 0 & +1 & 0 & +x_i & +2y_i & 0 & +x_i^2 & +2x_i y_i & +3y_i^2 & +x_i^3 & +3x_i y_i^2 \\ \vdots & & & & & & & & & & & \\ \vdots & & & & & & & & & & & \\ \cdots & \cdots & \cdots & \cdots & \cdots & \cdots & \cdots & \cdots & \cdots & \cdots & \cdots & \cdots \end{bmatrix} x \begin{Bmatrix} a_1 \\ a_2 \\ a_3 \\ \vdots \\ a_{12} \end{Bmatrix} \tag{4.7}$$

In compact matrix form, Equation (4.7) is expressed as

$$\{d\} = [C]\{a\} \tag{4.8}$$

where [***C***] is the 12 × 12 matrix on the right side Equation (4.7).

Therefore, the constants (*a*'s) can be solved by

$$\{a\} = [C]^{-1}\{d\} \tag{4.9}$$

Equation (4.6) can now be expressed as

$$\{\psi\} = [P][C]^{-1}\{d\} \tag{4.10}$$

or

$$\{\psi\} = [N]\{d\} \tag{4.11}$$

where $[N] = [P][C]^{-1}$ is the shape matrix.

4.3. The Strain (Curvature)/Displacement and Stress (Moment)/Curvature Relationships

The curvature matrix;

$$\{\kappa\} = \begin{Bmatrix} \kappa_x \\ \kappa_y \\ \kappa_{xy} \end{Bmatrix} = \begin{Bmatrix} -\dfrac{\partial^2 w}{\partial x^2} \\ -\dfrac{\partial^2 w}{\partial y^2} \\ -\dfrac{2\partial^2 w}{\partial x \partial y} \end{Bmatrix} \tag{4.12}$$

expressing in matrix form,

$$\{\kappa\} = [Q]\{a\} \tag{4.13}$$

where [***Q***] is the coefficient matrix multiplied by the a's in Equation (4.12). Using Equation (4.9) for $\{a\}$, the curvature matrix is expressed as

$$\{\kappa\} = [B]\{d\} \tag{4.14}$$

where

$$[B] = [Q][C]^{-1} \tag{4.15}$$

is the gradient matrix.The moment/curvature matrix for the plate is given by

$$\{M\} = \begin{Bmatrix} M_x \\ M_y \\ M_{xy} \end{Bmatrix} = [D] \begin{Bmatrix} \kappa_x \\ \kappa_y \\ \kappa_{xy} \end{Bmatrix} = [D][B]\{d\} \tag{4.16}$$

where the [***D***] matrix is the constitutive matrix given for isotropic materials by

$$[D] = \frac{Et^3}{12(1-\upsilon^2)} \begin{bmatrix} 1 & \upsilon & 0 \\ \upsilon & 1 & 0 \\ 0 & 0 & \frac{1-\upsilon}{2} \end{bmatrix} \tag{4.17}$$

4.4. The Element Stiffness Matrix and Equations

The stiffness matrix is given by the usual form of the stiffness matrix as

$$[k] = \iint [B]^T [D][B] dxdy \tag{4.18}$$

where [*B*] is defined by Equation (4.15) and [*D*] is defined by Equation (4.17) The stiffness matrix for the four-noded rectangular element is of order 12 × 12. When the system [*K*] matrix is formed, the values of this matrix can be calculated as follows;

$$\{F\} = [K]\{d\} \tag{4.19}$$

5. SOLUTION OF THICK PLATES BY FINITE ELEMENTS

5.1. Equations for Stress Resultants

If internal stresses are written in a matrix form; the following two equations can be obtained.

$$\{\sigma\} = [E]\{\varepsilon\} \tag{5.1}$$

Similary, matrix E may be partitioned into;

$$[E] = \begin{bmatrix} [E_k] & 0 \\ 0 & [E_y] \end{bmatrix} \tag{5.2}$$

in which $[E_k]$ is of size 3x3 and $[E_y]$ is of size 2x2.
Equation (5.1) can also be written in the following form.

$$\begin{Bmatrix} \sigma_x \\ \sigma_y \\ \tau_{xy} \\ \tau_{xz} \\ \tau_{yz} \end{Bmatrix} = \begin{bmatrix} \frac{E_x}{(1-v_{xy}v_{yx})} & \frac{v_{xy}E_x}{(1-v_{xy}v_{yx})} & 0 & 0 & 0 \\ \frac{v_{yx}E_y}{(1-v_{xy}v_{yx})} & \frac{E_y}{(1-v_{xy}v_{yx})} & 0 & 0 & 0 \\ 0 & 0 & \frac{E_x}{2(1+v_{xy})} & 0 & 0 \\ 0 & 0 & 0 & \frac{E_x}{2.4(1+v_{xz})} & 0 \\ 0 & 0 & 0 & 0 & \frac{E_y}{2.4(1+v_{yz})} \end{bmatrix} \begin{Bmatrix} \varepsilon_x \\ \varepsilon_y \\ \gamma_{xy} \\ \gamma_{xz} \\ \gamma_{yz} \end{Bmatrix} \tag{5.3}$$

if internal bending moments are written in a matrix form;

$$\{M\} = [D]\{\varepsilon\} \tag{5.4}$$

where D, the elasticity matrix, is given as;

$$[D] = \begin{bmatrix} \overline{E}_k & 0 \\ 0 & \overline{E}_y \end{bmatrix} \tag{5.5}$$

where

$$\begin{aligned} \overline{E}_k &= E_k \frac{t^3}{12} \\ \overline{E}_y &= k\, E_y\, t \end{aligned} \tag{5.6}$$

In this equation, k is a constant to account for the actual non-uniformity of the shearing stresses. Equation (5.4) can be written in terms of the internal stresses and strains, respectively, and it is given as;

$$\begin{Bmatrix} M_{xx} \\ M_{yy} \\ M_{xy} \\ Q_x \\ Q_y \end{Bmatrix} = \begin{Bmatrix} \int_{-t/2}^{t/2} \sigma_x z \\ \int_{-t/2}^{t/2} \sigma_y z \\ \int_{-t/2}^{t/2} \tau_{xy} z \\ \int_{-t/2}^{t/2} \tau_{xz} \\ \int_{-t/2}^{t/2} \tau_{yz} \end{Bmatrix} = [D] \begin{Bmatrix} \dfrac{\partial \phi_x}{\partial x} \\ -\dfrac{\partial \phi_y}{\partial y} \\ \left(\dfrac{\partial \phi_x}{\partial y} + \dfrac{\partial \phi_y}{\partial x} \right) \\ \phi_x + \dfrac{\partial w}{\partial x} \\ -\phi_y + \dfrac{\partial w}{\partial y} \end{Bmatrix} = [D] \begin{Bmatrix} \varepsilon_x \\ \varepsilon_y \\ \gamma_{xy} \\ \gamma_{xz} \\ \gamma_{yz} \end{Bmatrix} \tag{5.7}$$

5.2. Boundary conditions

For fixed supported plates;

Along $x = -a$ and $x = a$; $\quad \phi_x = 0$ and $w_0 = 0$

Along $y = -b$ and $y = b$; $\quad \phi_y = 0$ and $w_0 = 0$

For simply supported plates;

Along $x = -a$ and $x = a$; $\quad M_x = 0$ and $w_0 = 0$

Along $y = -b$ and $y = b$; $\quad M_x = 0$ and $w_0 = 0$

5.3. Finite Element Formulation of the Problem

For a rectangular plate-bending element the nodal displacements can be written as follows;

$$w_i = \{w, u, v\} = \{w, z\phi_x, -z\phi_y\} = \left\{w, z\frac{\partial \phi_i}{\partial x}, -z\frac{\partial \phi_i}{\partial_y}\right\} \tag{5.8}$$

$$w = \sum h_{i1} w_i \qquad u = z\phi_x = z\sum_1^4 h_{i2}\phi_{xi} \qquad vz\phi_y = -z\sum_1^4 h_{i3}\phi_{yi}\ ,\ (i = 1,2,3,4) \tag{5.9}$$

Nodal actions corresponding to the displacements in Equation (5.9) are;

$$p_i = \{p_{i1}, p_{i2}\, p_{i3}\} = \{p_{zi}, M_{xi}, M_{yi}\} \qquad (i = 1,2,3,4) \tag{5.10}$$

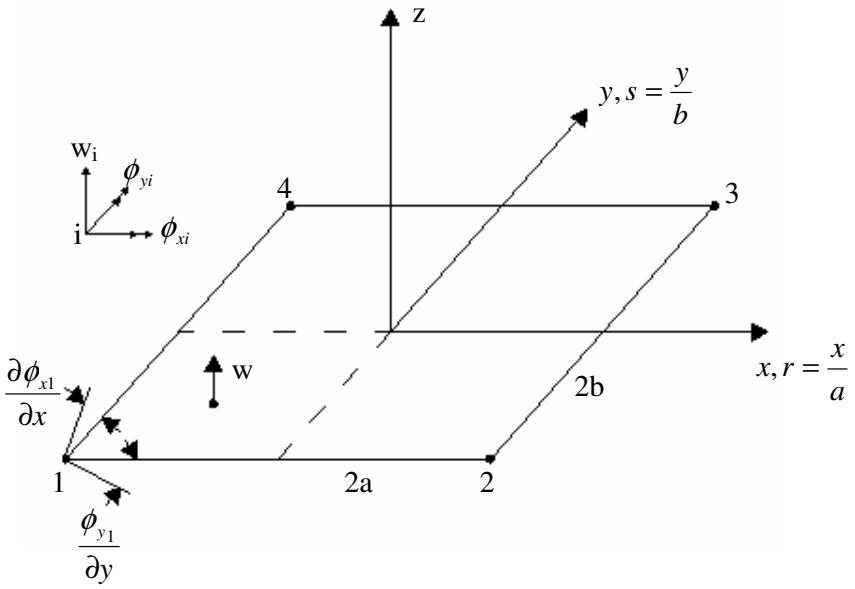

Figure 5.1. The finite element model for thick plate

The symbols p_{zi} denotes a force in the z direction, but M_{xi} and M_{yi} are moments in the x and y directions, respectively. Note that these fictitious moments at the nodes are not the same as the distributed moments in the vector M of generalized stresses [28].

The displacement function chosen for this element is;

$$w = c_1 + c_2 r + c_3 s + c_4 rs \tag{5.11}$$

which is a complete linear of four terms. From this assumption, it is possible to derive the displacement shape function to be;

$$\{h_i\} = \{h_1, h_2, h_3, h_4\} \tag{5.12}$$

where

$$\begin{aligned} h_1 &= 0.25\,(1+r)\,(1+s) \\ h_2 &= 0.25\,(1-r)\,(1+s) \\ h_3 &= 0.25\,(1-r)\,(1-s) \\ h_4 &= 0.25\,(1+r)\,(1-s) \end{aligned} \tag{5.13}$$

The 3x3 Jacobian matrix required in this formulation is,

$$[J] = \begin{bmatrix} 0 & x_r & y_r \\ 0 & x_s & y_s \\ 1 & 0 & 0 \end{bmatrix} \tag{5.14}$$

where

$$\begin{aligned} x_r &= \sum_{i=1}^{4} \left(h_{i,r} x_i \right) \\ y_r &= \sum_{i=1}^{4} \left(h_{i,r} y_i \right) \end{aligned} \tag{5.15}$$

$$x_s = \sum_{i=1}^{4} \left(h_{i,s} x_i \right)$$
$$y_s = \sum_{i=1}^{4} \left(h_{i,s} y_i \right)$$

The inverse of J becomes

$$J^{-1} = \begin{bmatrix} 0 & r_x & s_x \\ 0 & r_y & s_y \\ 1 & 0 & 0 \end{bmatrix} \tag{5.16}$$

We need certain derivatives with respect to local coordinates, which are placed into a 3x3 matrix, and it is given as;

$$\begin{bmatrix} w_r & u_r & v_r \\ w_s & u_s & v_s \\ w_z & u_z & v_z \end{bmatrix} = \sum_{i=1}^{4} \begin{bmatrix} f_{i,r} w_i & z f_{i,r} \phi_{xi} & -z f_{i,r} \phi_{yi} \\ f_{i,s} w_i & z f_{i,s} \phi_{xi} & -z f_{i,s} \phi_{yi} \\ 0 & f_i \phi_{xi} & -f_i \phi_{yi} \end{bmatrix} \tag{5.17}$$

Transformation of these derivatives to global coordinates is accomplished using the inverse of the Jacobian matrix and this transformation is given as follows;

$$\begin{bmatrix} w_x & u_x & v_x \\ w_y & u_y & v_y \\ w_z & u_z & v_z \end{bmatrix} = [J]^{-1} \begin{bmatrix} w_r & u_r & v_r \\ w_s & u_s & v_s \\ w_z & u_z & v_z \end{bmatrix} \tag{5.18}$$

The five types of nonzero strains to be considered for this element are;

$$\{\varepsilon\} = \begin{Bmatrix} \varepsilon_x \\ \varepsilon_y \\ \gamma_{xy} \\ \gamma_{xz} \\ \gamma_{yz} \end{Bmatrix} = \begin{Bmatrix} u_x \\ v_y \\ u_y + v_x \\ u_z + w_x \\ v_z + w_y \end{Bmatrix} \tag{5.19}$$

Stresses corresponding to the strains are given in equation (5.3). As a preliminary matter before formulating element stiffness matrix, matrix [B] partitioned and z factored from the upper part as follows;

$$[B]=\begin{bmatrix} B_k \\ B_\gamma \end{bmatrix}=\begin{bmatrix} z\overline{B}_k \\ B_\gamma \end{bmatrix} \tag{5.20}$$

where B_k has three rows and B_γ has two rows, then the stiffness matrix for this element is written as;

$$[K]=\int_v [B]^T[E][B]dV=\int_v \left[z\left[\overline{B_k}\right]^T \left[B_\gamma\right]^T\right]\begin{bmatrix} E_k & 0 \\ 0 & E_\gamma \end{bmatrix}\begin{bmatrix} z\left[\overline{B_k}\right]^T \\ \left[B_\gamma\right] \end{bmatrix}dV$$

$$[K]=\int_v \left(z^2\left[\overline{B_k}\right]^T[E_k]\left[\overline{B_k}\right]\right)+\left(\left[\overline{B_\gamma}\right]^T[E_\gamma]\left[\overline{B_\gamma}\right]\right)dV \tag{5.21}$$

Integration through the thickness yields;

$$[K]=\int_A \left[\overline{B_k}\right]^T\left[\overline{E_k}\right][B_k]+\left[\overline{B_\gamma}\right]^T\left[\overline{E_\gamma}\right]\left[\overline{B_\gamma}\right]dA \tag{5.22}$$

Thus,

$$[K]=\int_A \left[\overline{B}\right]^T\left[\overline{E}\right]\left[\overline{B}\right]dA=\int_{-1}^{1}\int_{-1}^{1}\left[\overline{B}\right]^T\left[\overline{E}\right]\left[\overline{B}\right][J]drds \tag{5.23}$$

which must be evaluated numerically [22]. The matrix that shows the displacements and rotations in the plate is given as follows;

$$\{d\}=\left[w_1\ \phi_x^1\ \phi_y^1;\ w_2\ \phi_x^2\ \phi_y^2;\ w_3\ \phi_x^3\ \phi_y^3;\ w_4\ \phi_x^4\ \phi_y^4\right] \tag{5.24}$$

and the values of this matrix can be calculated as follows;

$$\{F\} = [K]\{d\} \tag{5.25}$$

6. DEVELOPMENT OF A GRID FRAMEWORK MODEL

6.1. Introduction

In this chapter a rectangular grid framework model will be presented which will allow the numerical solution of the partial differential governing equation of the Kirchoff Plate Theory (Thin plates) and Mindlin Plate Theory (Thick plates). Because of the assumptions used in developing the basic elastic plate theory, it is necessary to consider only bending displacements in the development of the grid framework model. Therefore, a grid framework model can be developed by equating the displacements of the grid model to the actual displacements of a plate element subjected to bending and twisting moments. This grid framework model consists of six members – four perimeter beams, each capable of withstanding only out of plane bending. In this manner a rectangular grid model with five cross sectional properties will define uniquely a rectangular element of a plate [29].

6.2. Properties of a Plate Element

Consider the rectangular elastic plate element shown in *Figure 6.1-a,* which has exterior dimensions L and αL for the side lengths and h for thickness. When this plate element is subjected to bending moments M_1, as shown in *Figure 6.1-b*, the angular rotation in the direction of bending is given as

$$\theta_1 = \frac{\alpha L M_1}{E\left(\frac{t^3}{12}\right)} \tag{6.1}$$

where E is the modulus of elasticity of the material. Taking Poisson's ratio as ν, the angular rotation in the orthogonal direction is

$$\theta_2 = \frac{\nu L M_1}{E\left(\frac{t^3}{12}\right)} \tag{6.2}$$

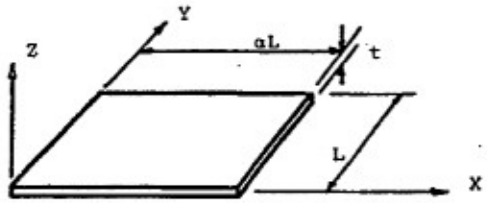

(a) Dimension of elastic plate element

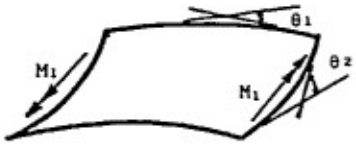

(b) Application of Bending Moment M_1

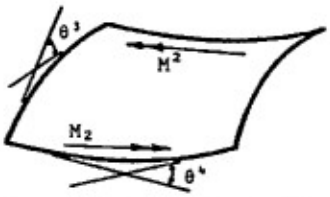

(c) Application of Bending Moment M_2

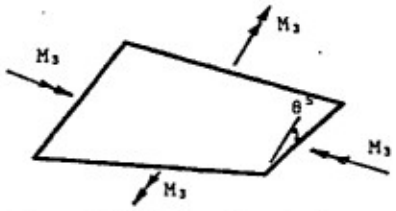

(d) Application of Twisting Moment M_3

Figure 6.1. General elastic plate element

Similarly, when the element is subjected to bending moments M_2 along the other two edges, as shown in *Figure 6.1-c*, the angular rotation about the X and Y axes are given by

$$\theta_3 = \frac{LM_2}{E\left(\frac{t^3}{12}\right)} \tag{6.3}$$

and

$$\theta_4 = \frac{\nu\alpha LM_2}{E\left(\frac{t^3}{12}\right)} \tag{6.4}$$

Finally if twisting moments of intensity M_3 are applied to all edges of the element as in *Figure 6.1-d*, the resulting angle of twist will be

$$\theta_5 = \frac{\alpha LM_3(1+\nu)}{E\left(\frac{t^3}{12}\right)} \tag{6.5}$$

Therefore, the deformations of a general plate element subjected to bending and twisting moments are known.

6.3. Development of the Stiffness Equation for the Equivalent Grid

An equivalent grid model of the plate element can be constructed of six members. The physical properties of the grid members can be determined by equating the rotation of the grid nodes with those of the same size plate element. It is important that both the plate element and the equivalent grid structure be subjected to statically equivalent loads.

Consider, for example, a structural grid as shown in *Figure 6.2-a* composed of six members. The physical dimensions of the grid are L and αL as the lengths of the edge members and βL as the length of the diagonals. The two end members of length L have moments of inertia about their Y axis designated as I_e and torsional constants designated as GJ_e/E. Similarly, the two side members have moments of inertia and torsional constants

equal to I_s and GJ_s/E respectively. The diagonal members are assumed to resist no torsion but have a moment of inertia equal to I_d.

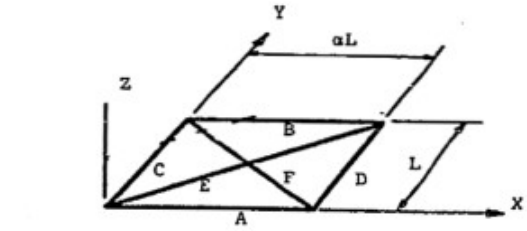

(a) Dimension of equivalent grid structure

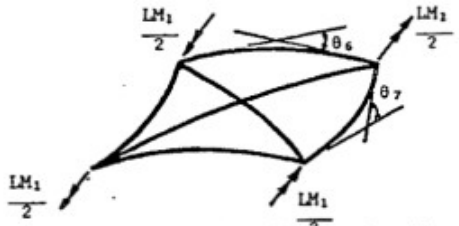

(b) Applications of equivalent bending moments M_1

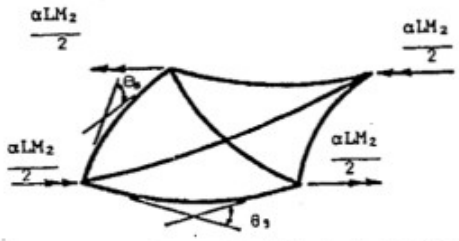

(c) Applications of equivalent bending moments M_2

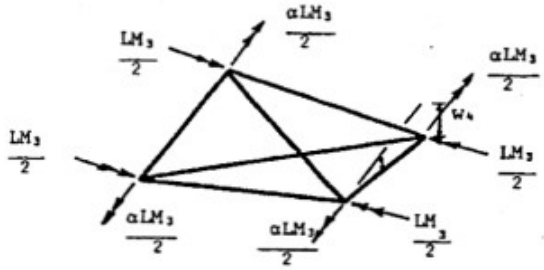

(d) Applications of equivalent twisting moments M_3

Figure 6.2. Equivalent grid structure

The joint stiffness matrix for the complete system can now be formulated by substituting the above member properties into the general grid member stiffness matrix and then assembling all of the resulting stiffness influence coefficients into the joint stiffness matrix. The location of the stiffness influence coefficients in the joint stiffness matrix is determined by the number of the deformation causing the action to occur. At each joint of the model structure, three deformations and three corresponding actions can occur.

Once the member stiffness matrices are complete, the joint stiffness matrix, and the governing stiffness equation, can be assembled.

6.4. Solution of the Equivalent Grid Stiffness Equation

In order to obtain the physical constants of the equivalent grid framework members such that the model represents the actions of a plate element, the deformations of the grid framework model are equated to the corresponding deformations of the plate element.

$$\{A\} = [K]\{D\} \tag{6.6}$$

Where

$\{A\}$ = Actions of the plate element

$[K]$ = Total stiffress matrix

$\{D\}$ = Displacement and Rotations vector

The deformations of the grid model may be found by solving *Equation 6.6* when the model is alternately subjected to loads $LM_1/2$, $\alpha LM_2/2$ and the twisting moments as shown in *Figures 6.2-b, 6.2-c* and *6.2-d*. For each loading condition, two independent simultaneous equations are formed from the matrix relationships of *Equation 6.6.* By equating these independent equations, expressions are obtained for the deformations of the grid framework model in terms of the unknown member properties as

$$\theta_6 = \frac{L^2 M_1 \alpha}{2E} \times \frac{\beta^3 I_e + I_d}{\beta^3 I_e I_s + I_d I_s + \alpha^3 I_d I_e} \tag{6.7}$$

$$\theta_7 = \frac{L^2 M_1 \alpha^2}{2E} \times \frac{I_d}{\beta^3 I_e I_s + I_d I_s + \alpha^3 I_d I_e} \tag{6.8}$$

$$\theta_8 = \frac{L^2 M_2 \alpha}{2E} \times \frac{\beta^3 I_s + \alpha^3 I_d}{\beta^3 I_e I_s + I_d I_s + \alpha^3 I_d I_e} \tag{6.9}$$

$$\theta_9 = \frac{L^2 M_2 \alpha^3}{2E} \times \frac{I_d}{\beta^3 I_e I_s + I_d I_s + \alpha^3 I_d I_e} \tag{6.10}$$

$$\theta_{10} = \frac{L^2 M_3 \beta^3 \alpha}{2E\left[\beta^3\left(\frac{GJ_s}{E}\right) + 2\alpha I_d\right]} \tag{6.11}$$

and

$$w_4 = -L\theta_{10} \tag{6.12}$$

Equating corresponding deformations, it can be seen that

$$\theta_1 = \theta_6 \tag{6.13}$$

$$\theta_2 = \theta_7 \tag{6.14}$$

$$\theta_3 = \theta_8 \tag{6.15}$$

$$\theta_4 = \theta_9 \tag{6.16}$$

and

$$\theta_5 = \theta_{10} \tag{6.17}$$

Expanding and solving Equations (6-13) through (6-17), the final beam properties are computed as

$$I_e = \frac{(\alpha^2 - \nu)L}{2\alpha(1-\nu^2)}\frac{t^3}{12} \tag{6.18}$$

$$I_s = \frac{(1-\alpha^2\nu)L}{2(1-\nu^2)}\frac{t^3}{12} \tag{6.19}$$

$$I_d = \frac{\nu\beta^3 L}{2\alpha(1-\nu^2)}\frac{t^3}{12} \tag{6.20}$$

$$\frac{GJ_s}{E} = \frac{(1-3\nu)L}{2(1-\nu^2)}\frac{t^3}{12} \tag{6.21}$$

$$\frac{GJ_e}{E} = \frac{\alpha(1-3\nu)L}{2(1-\nu^2)}\frac{t^3}{12} \tag{6.22}$$

Using Equations (6-18) through (6-22), a plate may be idealized into an equivalent grid framework model which, when analysed by any standard frame or grid analysis computer program, will represent the actions of the original plate structure [29].

6.5. Influence of Shear Deformations

The influence of shear deformations is best included in a stiffness matrix, by means of λ–shear correction factors [30], which actually modify the flexural rigidities as follows:

$$A_i = \frac{4EI}{L}\lambda_i \tag{6.23}$$

$$B_i = \frac{2EI}{L}\lambda_{ij} \tag{6.24}$$

where

$$\lambda_i = 0.75\,\varepsilon + 0.25 \tag{6.25}$$

$$\lambda_{ij} = 1.50\,\varepsilon - 0.5 \tag{6.26}$$

$$\varepsilon = 1/(1+\gamma) \tag{6.27}$$

$$\gamma = 24\,k_s\,(1+\nu)\;I/(L^2 F) \tag{6.28}$$

k_s = Shape factor

F = Cross-sectional area

I = Moment of inertia

ν = Poisson's ratio,

for plates with constant thickness, the ratio I/F may be replaced by $t^2/12$, hence,

$$\gamma = 24\, k_s\, (1+\nu)\; t^2/(12\, L^2) \tag{6.29}$$

When the above correction factors, λ, are multiplied by the appropriate flexural stiffness values, A_i, A_j and B of the lattice elements, the shear deformations are duly taken into account without any approximations [31]. Therefore, the stiffness matrix of a rectangular element given, is ideally suitable for the flexural analysis of thick plates in which, the thickness to span ratio exceeds 1/10.

In order to neglect the influence of shear deformations in plate bending, it is sufficient to take the correction factor $\gamma = 0$, which virtually amounts to taking $\varepsilon = 1$.

The stiffness matrix of a grid element, as described elsewhere in detail by Tezcan [30] is utilized with a code number technique and appropriate direction cosines to obtain the 12 by 12 master stiffness matrix of the lattice model. The appropriate lengths and rigidities for different bars of a typical rectangular lattice model, are listed in Table 6.1. The 12 by 12 stiffness matrix of the entire lattice model is presented in three separate parts in Tables 6.2 to 6.4.

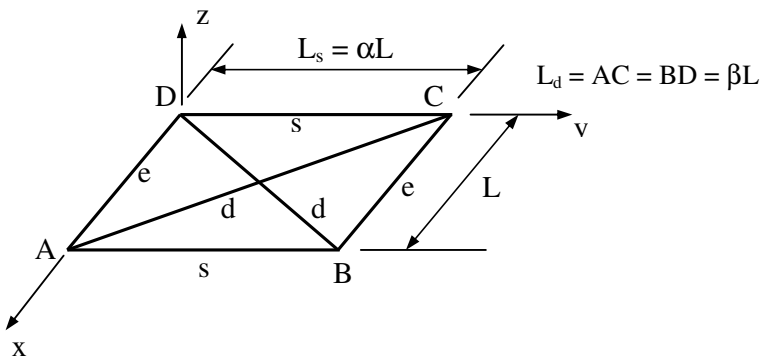

Figure 6.3. Typical lattice element

Table 6.1. Flexural stiffness of lattice bars

HORIZONTAL BEAMS $L_s = \alpha L$	SIDE BEAMS $L_e = L$	DIAGONALS $L_d = \beta L$
$A_s = \frac{4EI_s}{\alpha L}\lambda_{i,s}$ $B_s = \frac{2EI_s}{\alpha L}\lambda_{ij,s}$ $C_s = \frac{A_s + B_s}{\alpha L}$ $D_s = 2C_s/(\alpha L)$ $T_s = GJ_s/(\alpha L)$	$A_e = \frac{4EI_e}{L}\lambda_{i,e}$ $B_e = \frac{2EI_e}{L}\lambda_{ij,e}$ $C_e = \frac{A_e + B_e}{L}$ $D_e = 2C_e / L$ $T_e = GJ_e / L$	$A_d = \frac{4EI_d}{\beta L}\lambda_{i,d}$ $B_d = \frac{2EI_d}{\beta L}\lambda_{ij,d}$ $C_d = \frac{A_d + B_d}{\beta L}$ $D_d = 2C_d / \beta L$ $T_d = 0$
$\lambda_{i,s} = 0.75\varepsilon_s + 0.25$ $\lambda_{ij,s} = 1.5\varepsilon_s - 0.5$ $\varepsilon_s = 1/(1+\gamma_s)$ $\gamma_s = \frac{24k_s(1+\nu)}{\alpha^2 L^2}\frac{t^2}{12}$ $\frac{I_s}{F_s} = \frac{t^2}{12}$	$\lambda_{i,e} = 0.75\varepsilon_e + 0.25$ $\lambda_{ij,e} = 1.5\varepsilon_e - 0.50$ $\varepsilon_e = 1/(1+\gamma_e)$ $\gamma_e = \frac{24k_s(1+\nu)}{L^2}\frac{t^2}{12}$ $\frac{I_e}{F_e} = \frac{t^2}{12}$	$\lambda_{i,d} = 0.75\varepsilon_d + 0.25$ $\lambda_{ij,d} = 1.5\varepsilon_d - 0.5$ $\varepsilon_d = 1/(1+\gamma_d)$ $\gamma_d = \frac{24k_s(1+\nu)}{\beta^2 L^2}\frac{t^2}{12}$ $\frac{I_d}{F_d} = \frac{t^2}{12}$
$\beta = \sqrt{1+\alpha^2}$		

Table 6.2. Upper left portion of the stiffness matrix ($[k]_1$)

$[k]_{XYZ}$ = (12 x 12)

k_1 (6x6)	k_3^T (6x6)
k_3 (6x6)	k_2 (6x6)

$[k]_1$ =

$D_s + D_d + D_e$	$-C_s - mC_d$	$-lC_d - C_e$	$-D_s$	$-C_s$	0
$-C_s - mC_d$	$m^2 A_d + l^2 T_d$ $A_s + T_e$	$-lmA_d$ $+ lmT_d$	C_s	B_s	0
$-lC_d + C_e$	$-lmA_d + lmT_d$	$T_s + l^2 A_d +$ $m^2 T_d + A_e$	0	0	$-T_s$
$-D_s$	C_s	0	$D_s + D_e +$ D_d	$C_s + mC_d$	$C_e + lC_d$
$-C_s$	B_s	0	$C_s + mC_d$	$T_e + m^2 A_d$ $l^2 T_d + A_s$	$lmA_d - lmT_d$
0	0	$-T_s$	$C_e + lC_d$	$lmA_d + lmT_d$	$A_e + l^2 A_d +$ $m^2 T_d + T_s$

l: direction cosine with respect to x-axis
m: direction cosine with respect to y-axis

Table 6.3. Lower right portion of the stiffness matrix ($[k]_2$)

$[k]_2 =$

$D_e + D_s + D_d$	$-C_s - mC_d$	$-C_e - lC_d$	$-D_s$	$-C_s$	0
$-C_s - mC_d$	$T_e + m^2 A_d + l^2 T_d + A_s$	$lmA_d - lmT_d$	C_s	B_s	0
$-C_e - lC_s$	$lmA_d - lmT_d$	$A_e + l^2 A_d + m^2 T_d + T_s$	0	0	$-T_c$
$-D_s$	C_s	0	$D_e + D_s + D_d$	$C_s + mC_d$	$-C_e - lC_d$
$-C_s$	B_s	0	$C_s + mC_d$	$T_e + m^2 A_d + l^2 T_d + A_s$	$-lmA_d - lmT_d$
0	0	$-T_s$	$-C_e - lC_d$	$-lmA_d + lmT_d$	$A_e + l^2 A_d + m^2 T_d + T_s$

Table 6.4. Lower left portion of the stiffness matrix ($[k]_3$)

$[k]_3 =$

$-D_e$	0	$-C_e$	$-D_d$	$-mC_d$	$-lC_d$
0	$-T_e$	0	mC_d	$m^2 B_d - l^2 T_d$	$lmB_d + lmT_d$
C_e	0	B_e	lC_d	$lmB_d + lmT_d$	$l^2 B_d - m^2 T_d$
$-D_d$	mC_d	$-lC_d$	$-D_e$	0	$-C_e$
$-mC_d$	$m^2 B_d - l^2 T_d$	$-lmB_d - lmT_d$	0	$-T_e$	0
lC_d	$-lmB_d - lmT_d$	$l^2 B_d - m^2 T_d$	C_e	0	B_e

Table 6.5. Direction cosines, *l* and *m*

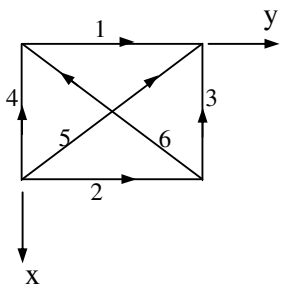

Bar No	*l*	*m*
1, 2	0	1
3, 4	1	0
5	$-1/\beta$	α/β
6	$1/\beta$	α/β

A given plate bending problem, requires idealisation of the plate geometry into a suitable assembly of small rectangular lattice models. By applying a suitable correction factor, k_s, to the idealised grid framework the shear deformations also are included in the lattice model. After a direct stiffness method of analysis, the computer output normally contains the direct forces and moments at the corner points of each rectangular lattice.

It is normally sufficient to add the corner forces and moments of the two adjacent rectangles, at a particular cross section, and then to divide this sum by the tributary distance, in order to obtain the corresponding shears and moments of the plate for a unit strip.

7. ILLUSTRATIVE EXAMPLES

7.1. Square Plate Model

7.1.1. Model Description

In order to utilize the influence of shear deformations in plate bending, a square plate model is used. The plate is investigated for clamped (fixed) support and hinge support cases around the plate.

A square plate size 8m x 8m is chosen in order to ease and simplify the calculations and only to concentrate on shear deformations. The Poisson's ratio ν is taken as 0.3 .The modulus of elasticity is taken as $E = 3\ 10^7$ kN/m^2. The analysis is conducted for the loading cases of $q = 50$ kN/m^2 uniformly distributed load and $P = 3200$ kN point load at the center.

Due to two way symmetry only ¼ of the plate is analysed, decreasing the time for solutions. The plate model is analysed for different t/L ratios to monitor the influence shear deformations due to thickness to length ratio increase. The t/L ratio analysed starts from t/L = 0.01 and goes up to t/L = 1. In other words keeping the plate dimensions constant thicknesses from 0.08 m up to 8 m are analysed.

In order to analyse the plate, the LUSAS [32] package program, a general finite element analysis program, is used for all support and loading conditions mentioned above.

Modulus of elasticity, $E = 3.10^7$ kN/m^2

Poisson's ratio, $\nu = 0.3$

Uniformly distributed load, $q = 50$ kN/m^2

Point load at center: $P = 3200$ kN

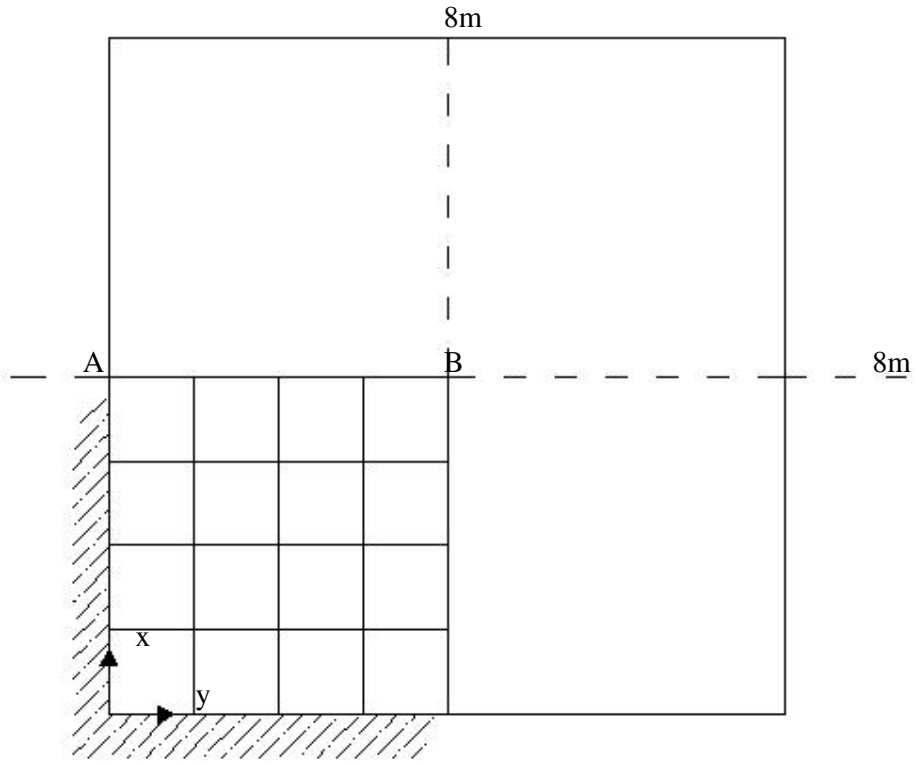

Figure 7.1. The square plate model

7.1.2. Thin Plate Model

The QF4 [33], 4-Node isoflex family of thin plate elements are assigned to the model. The QF4 elements are from a family of thin plate flexure elements in 2D with higher order models capable of modelling curved boundaries. The element formulation takes account of varying thickness and anisotropic properties. As required by thin plate theory transverse shearing effects are excluded. The degree of freedoms of the plate element is w, θ_x, θ_y at the corner nodes.

The model is loaded by the specified loading (Uniformly distributed and point loading at the center) to the fixed and simply supported boundary condition cases and the corresponding transverse displacement are noted.

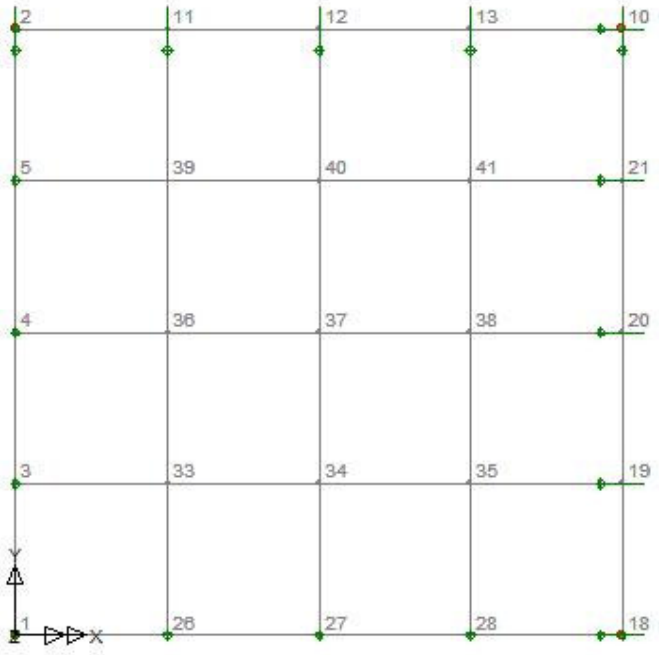

Figure 7.2. Thin plate element QF4 and node numbers

Exact Solutions for the vertical deflections and the bending moments in x and y-directions at the center of the plate are determined by means of the equations as follows: The central vertical deflection of the fixed supported square plate for the point load at the center is equal to [23] :

$$(W)_{x=a/2,y=a/2} = 0.0056 \ \frac{Pa^2}{D} \tag{7.1}$$

Where

$$D = \frac{Et^3}{12(1-\nu^2)} \tag{7.2}$$

The central vertical deflection for the Uniform Loading Case is equal to

$$(W)_{x=a/2,y=a/2} = 0.00126 \ \frac{qa^4}{D} \tag{7.3}$$

The central vertical deflection of the fixed supported square plate for the point load at the center is equal to:

$$(W)_{x=a/2,y=a/2} = 0.0116 \quad \frac{Pa^2}{D} \tag{7.4}$$

The central vertical deflection for the uniform loading case is equal to

$$(W)_{x=a/2,y=a/2} = 0.0406 \quad \frac{qa^4}{D} \tag{7.5}$$

7.1.3. Thick Plate Elements

QTF8 element of *LUSAS* is a family of thick plate flexure elements based on a Mindlin plate formulation which assumes that

i) Normal stress in the transverse stress is negligible in comparison with the in plane stress
ii) "Normals" to the mid-surface remain straight but not necessarily normal to the mid-surface after deformation *(Figure 2.1).*

Thus the elements account for the transverse shear effects associated with thicker plates and the elements are termed "thick" plate elements.

The degree of freedoms are w, θ_x, θ_y at each node where θ_x and θ_y are the rotation of the normals to the mid-surface and include the effect of shear deformations.

The model is run for uniformly distributed load and point load, and for fixed and simply supported cases for the various t/L ratios and the corresponding center deflections are noted.

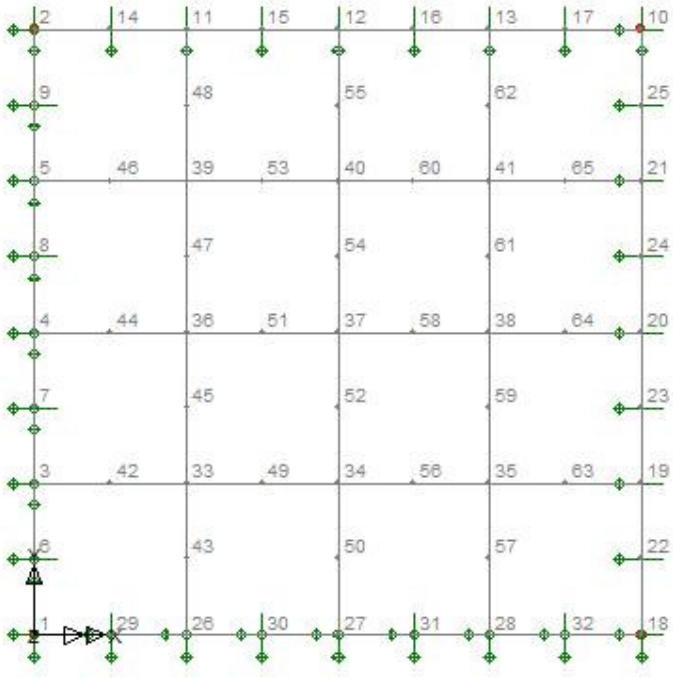

Figure 7.3. The Mindlin plate element QTF8 and node numbers

7.1.4. Grid Framework (Hrennikoff) Plate Model

The plate is also modelled using Hrennikoff grid framework method. The lattice elements are formed by dividing the one quarter of the plate analysed to 16 equal elements. The model obtained is given in *Figure 7.4* and the lattice element properties for the thin plate model are given in *Table 7.1*.

The same loading and support conditions are analysed for the varying t/L ratios as it is done with the 2D continuum elements mentioned above and the corresponding center displacement values are calculated.

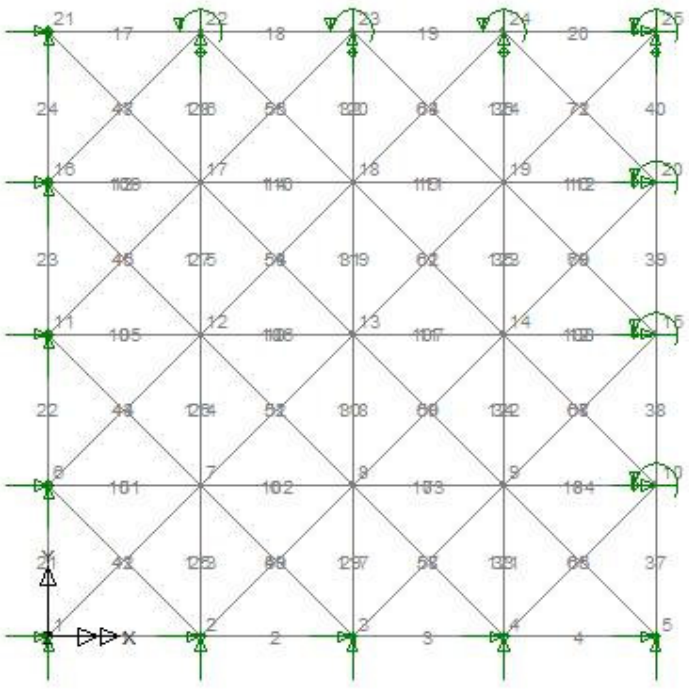

Figure 7.4. Lattice model, node and element numbers,

Table 7.1. Lattice element properties for the thin plate model

t/L	t *(m)*	Horizontal and Side Elements			Diagonal Element		
		Area (m^2)	I (m^4)	J (m^4)	Area (m^2)	I (m^4)	J (m^4)
0.01	0.08	0.030	$1.641\ 10^{-5}$	$2.344\ 10^{-7}$	0.042	$1.989\ 10^{-5}$	0
0.05	0.40	0.150	$2.051\ 10^{-3}$	$2.930\ 10^{-4}$	0.212	$2.487\ 10^{-3}$	0
0.1	0.80	0.300	$1.641\ 10^{-2}$	$2.344\ 10^{-4}$	0.424	$1.989\ 10^{-2}$	0
0.2	1.60	0.600	$1.313\ 10^{-1}$	$1.875\ 10^{-2}$	0.849	$1.591\ 10^{-1}$	0
0.3	2.40	0.900	$4.431\ 10^{-1}$	$6.330\ 10^{-2}$	1.273	$5.371\ 10^{-1}$	0
0.4	3.20	1.200	1.050	$1.500\ 10^{-1}$	1.697	1.273	0
0.5	4.00	1.500	2.051	$2.930\ 10^{-1}$	2.121	2.487	0
0.75	6.00	2.250	6.923	$9.890\ 10^{-1}$	3.182	8.392	0
1	8.00	3.000	16.41	2.344	4.243	19.89	0

7.1.5. Grid Framework Including Shear Deformations

The same model is used also for the grid framework plate model where shear deformations are included. The shear deformations are included by using appropriate shear correction factors for different loading cases. For the uniformly distributed load case the shape factor is found to be k_s, = 1.8. For the point loads, however, the appropriate shape factor is k_s, = 2.25, since in the point loading case the shear deformations are more pronounced.

7.1.6. 3D Model

The plate is also modelled using LUSAS 3D linear hexahedral stress element HX8M. Same loading and support conditions are applied to the 3D plate element model. Meshes for the elements are given in Table 7.2 and for the thickness to span ratio 0.3 the mesh of the plate model is given in Figure 7.5.

Table 7.2. Mesh sizes for square plate for 3D model

t/L	t *(m)*	**x-direction Mesh**	**y-direction Mesh**	**z-direction Mesh**
0.1	0.8	24	24	6
0.2	1.6	16	16	4
0.3	2.4	16	16	4
0.4	3.2	8	8	4
0.5	4.0	8	8	4
0.75	6.0	8	8	6
1	8.0	8	8	8

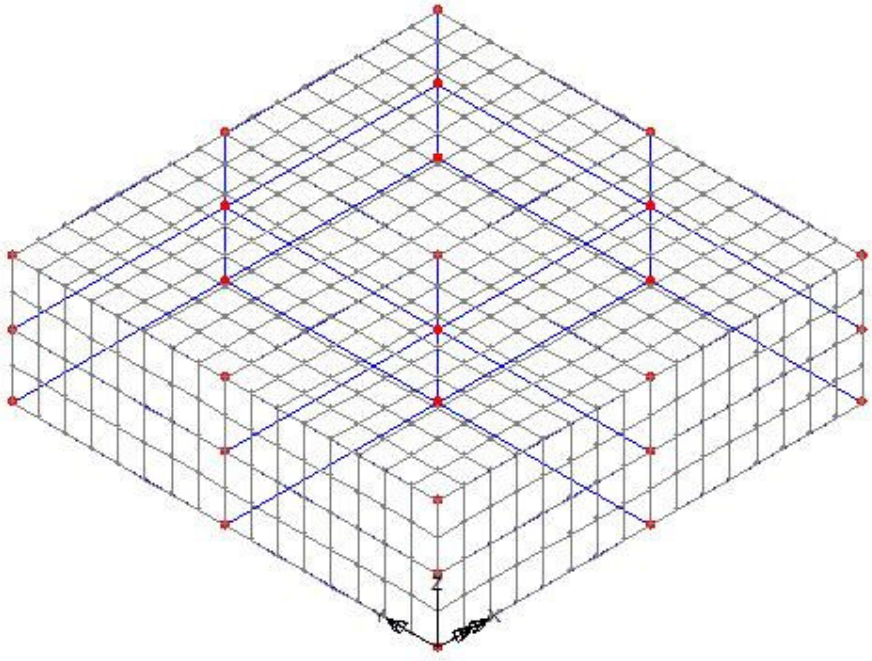

Figure 7.5 3D model mesh for t/L = 0.3

7.1.7. Results

The results obtained from LUSAS package program is presented for 4 different cases; fixed support and uniformly distributed load, fixed support and point load, simply supported and uniformly distributed load and finally simply supported and point load at the center. The displacements of all plate models, 2D continuum thin and thick plate models, lattice thin and thick plate models, are given in *Tables 7.3 to 7.6*. Also the plate is analysed for 3D stress conditions using 3D continuum solid elements and the results are presented.

The displacements are normalized by D/qL^4 for the uniformly distributed cases and D/PL^2 for the point loading cases in order to show clearly the effect of shear deformations and remove the effect of decreasing displacements in value with increasing thickness of the plate, since the loading is kept constant.

The displacements are also plotted for easy monitoring and given in *Figures 7.6 to 7.9*. The results obtained from the exact theory of thin plates are taken as basis and the deviation from the exact theory of thin plates are plotted. In other words the displacement values are divided by the exact theory and the ratios are plotted. From these figures it can easily be seen that the deviation from the thin plate theory becomes significant when the t/L ratio of the plate is bigger than 1/10.

From the *Figures 7.6* to *7.9* it can be seen that, the 2D continuum element and lattice model for thin plate is exactly matching with the exact theory. The Mindlin 2D plate element and 3D model start deviating from thin plate theory when the t/L ratio reaches 1/10. Moreover, for the fixed case at t/L = 0.5 the deflections are calculated as five times bigger than the condition when the shear deflection is neglected.

From the *Figures 7.6* to *7.9* it can easily be seen that the grid framework method defined herein is perfectly overlapping with the Mindlin plate element displacements for all loading cases and support cases with appropriate shear correction factors. With this finding it can be stated that the thick plate model considering shear deformation theory with complicated formulation can also be modelled with simple elements.

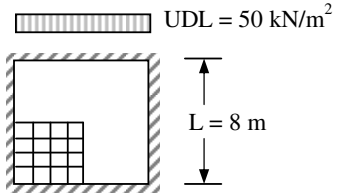

Table 7.3. Midspan deflection of a square fixed plate with UDL

$w = r\, D / q\, L^4$

t *(m)*	t / L	Normalized by D/qa^4					
		Exact (Thin plate)	**Thin Plate**[(1)] (4x4)	**Mindlin Plate**[(2)] (4x4)	**3D-FEM**	**Gridwork Thin Plate**	**Gridwork Thick Plate $k_s = 1.8$**
0.08	0.01	0.001260	0.001261	0.001258	-	0.001294	0.001290
0.4	0.05	0.001260	0.001261	0.001327	-	0.001294	0.001352
0.8	0.1	0.001260	0.001261	0.001505	0.001511	0.001294	0.001532
1.6	0.2	0.001260	0.001261	0.002173	0.002086	0.001298	0.002203
2.4	0.3	0.001260	0.001261	0.003245	0.003117	0.001299	0.003282
3.2	0.4	0.001260	0.001261	0.004730	0.004620	0.001296	0.004777
4	0.5	0.001260	0.001261	0.006631	0.006565	0.001297	0.006690
6	0.75	0.001260	0.001261	0.013215	0.013902	0.001302	0.013317
8	1.0	0.001260	0.001261	0.022424	0.028571	0.001308	0.022582

(1) LUSAS Program QF4 Thin Plate Element

(2) LUSAS Program QTF8 Thick Plate (Mindlin) Element

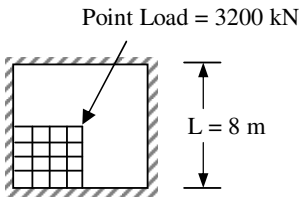

Table 7.4. Midspan deflection of a square fixed plate with point loading

$w = r\ D / P\ L^2$

t ***(m)***	**t / L**	**Normalized by D/Pa^2**					
		Exact (Thin plate)	**Thin Plate**[(1)] (4x4)	**Mindlin Plate**[(2)] (4x4)	**3D-FEM**	**Gridwork Thin Plate**	**Gridwork Thick Plate $k_s = 2.25$**
0.08	0.01	0.005600	0.005573	0.005570	-	0.005741	0.005732
0.4	0.05	0.005600	0.005573	0.006107	-	0.005743	0.006250
0.8	0.1	0.005600	0.005573	0.007637	0.009286	0.005742	0.007793
1.6	0.2	0.005600	0.005571	0.013643	0.018890	0.005775	0.013747
2.4	0.3	0.005600	0.005572	0.023551	0.046434	0.005769	0.023551
3.2	0.4	0.005600	0.005574	0.037363	0.053099	0.005757	0.037226
4	0.5	0.005600	0.005573	0.055100	0.094437	0.005766	0.054782
6	0.75	0.005600	0.005572	0.116653	0.289257	0.005798	0.115610
8	1.0	0.005600	0.005573	0.202816	0.664560	0.005839	0.200962

(1) LUSAS Program QF4 Thin Plate Element

(2) LUSAS Program QTF8 Thick Plate (Mindlin) Element

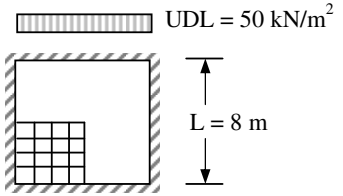

Table 7.5. Midspan deflection of a square simply supported plate with UDL

$w = r\ D / q\ a^4$

t ***(m)***	**t / L**	**Normalized by D/qa^4**					
		Exact (Thin plate)	**Thin Plate**[(1)] (4x4)	**Mindlin Plate**[(2)] (4x4)	**3D-FEM**	**Gridwork Thin Plate**	**Gridwork Thick Plate k_s = 1.8**
0.08	0.01	0.004060	0.003966	0.004106	-	0.004229	0.004188
0.4	0.05	0.004060	0.003966	0.004289	-	0.004229	0.004286
0.8	0.1	0.004060	0.003966	0.004617	0.004602	0.004229	0.004561
1.6	0.2	0.004060	0.003966	0.005544	0.005547	0.004236	0.005476
2.4	0.3	0.004060	0.003967	0.006822	0.007119	0.004258	0.006787
3.2	0.4	0.004060	0.003966	0.008457	0.008919	0.004232	0.008473
4	0.5	0.004060	0.003966	0.010465	0.012929	0.004234	0.010530
6	0.75	0.004060	0.003967	0.017208	0.026877	0.004242	0.017376
8	1.0	0.004060	0.003966	0.026490	0.053654	0.004251	0.026758

(1) LUSAS Program QF4 Thin Plate Element

(2) LUSAS Program QTF8 Thick Plate (Mindlin) Element

Table 7.6. Midspan deflection of a square simply supported plate with point loading

$w = r\ D / P\ a^2$

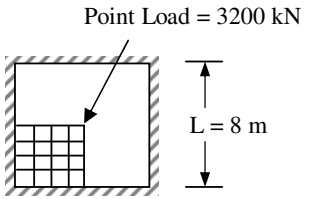

t *(m)*	t / L	Normalized by D/Pa^2					
		Exact (Thin plate)	**Thin Plate**[1] (4x4)	**Mindlin Plate**[2] (4x4)	**3D-FEM**	**Gridwork Thin Plate**	**Gridwork Thick Plate $k_s = 2.25$**
0.08	0.01	0.011600	0.011573	0.011669	-	0.012262	0.012166
0.4	0.05	0.011600	0.011573	0.012440	-	0.012265	0.007836
0.8	0.1	0.011600	0.011573	0.014286	0.016071	0.012263	0.014560
1.6	0.2	0.011600	0.011571	0.020835	0.026538	0.012302	0.021121
2.4	0.3	0.011600	0.011573	0.031172	0.055346	0.012347	0.031469
3.2	0.4	0.011600	0.011574	0.045275	0.063121	0.012280	0.045582
4	0.5	0.011600	0.011573	0.063255	0.106302	0.012294	0.063436
6	0.75	0.011600	0.011573	0.125143	0.310032	0.012329	0.124824
8	1.0	0.011600	0.011573	0.211401	0.706044	0.012376	0.210302

[1] LUSAS Program QF4 Thin Plate Element

[2] LUSAS Program QTF8 Thick Plate (Mindlin) Element

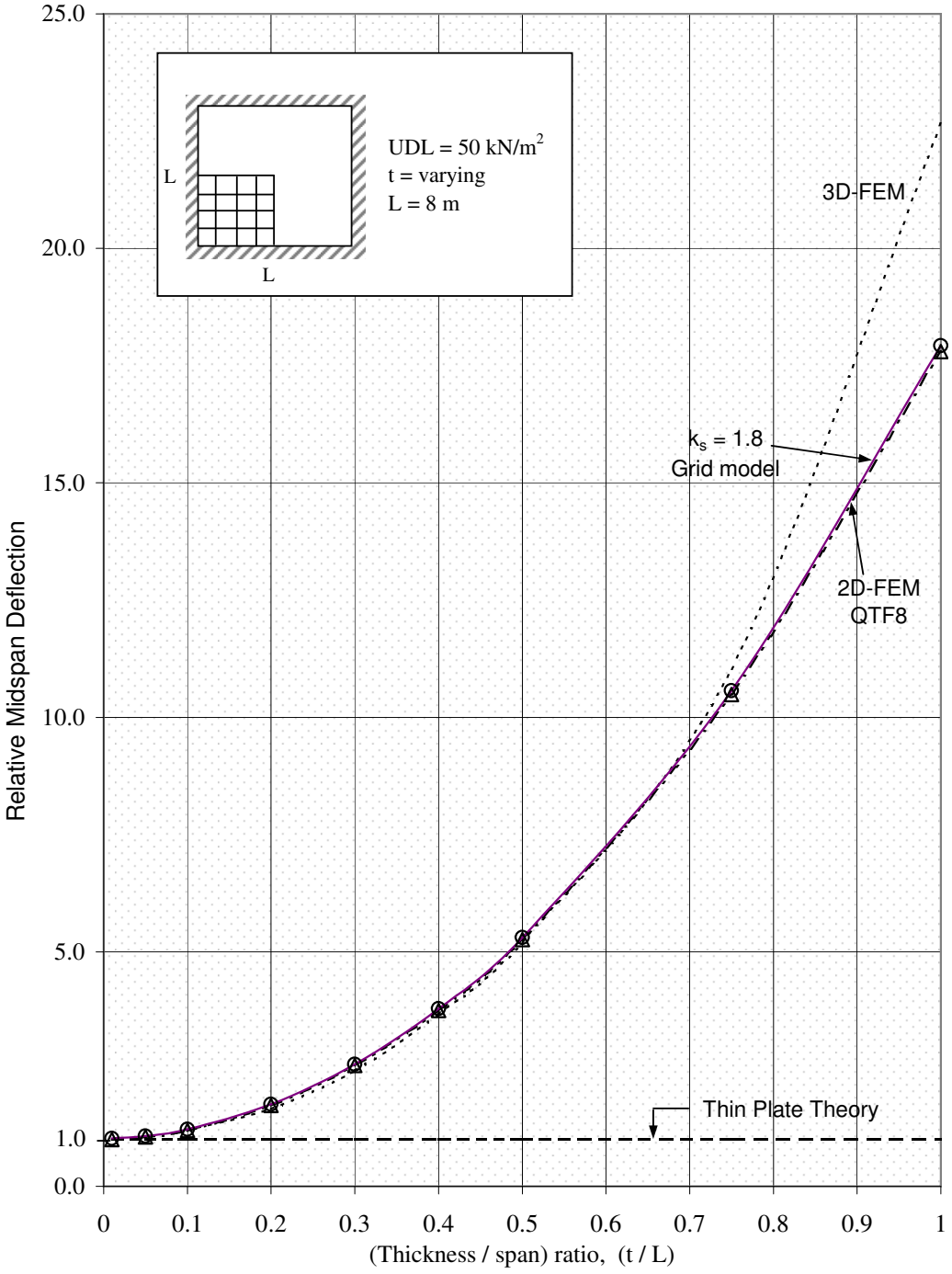

Figure 7.6. Midspan deflections of a square plate for fixed case - UDL
Thin plate theory deflection is assumed unity

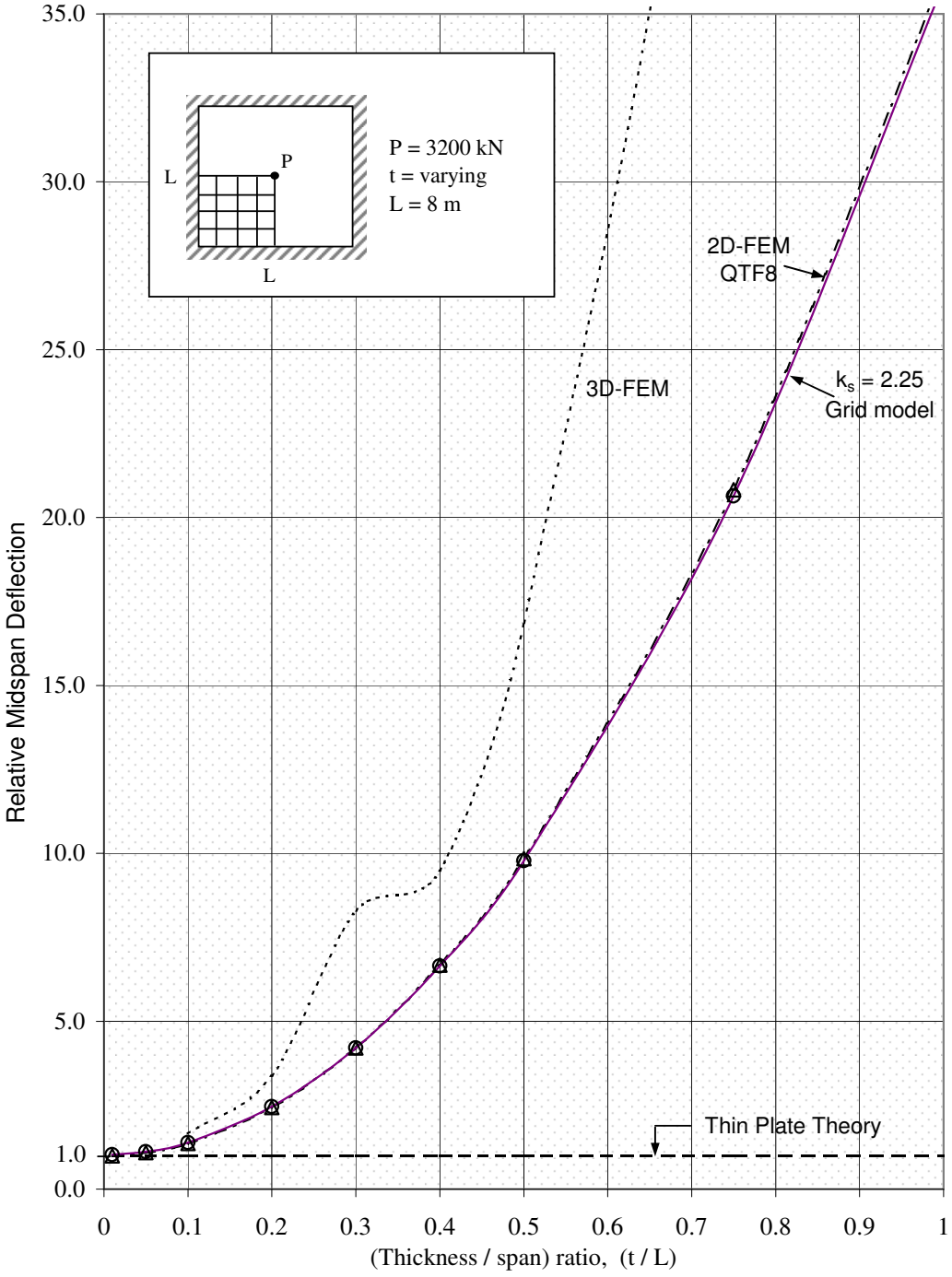

Figure 7.7. Midspan deflections of a square plate for fixed case - Point Loading
Thin plate theory deflection is assumed unity

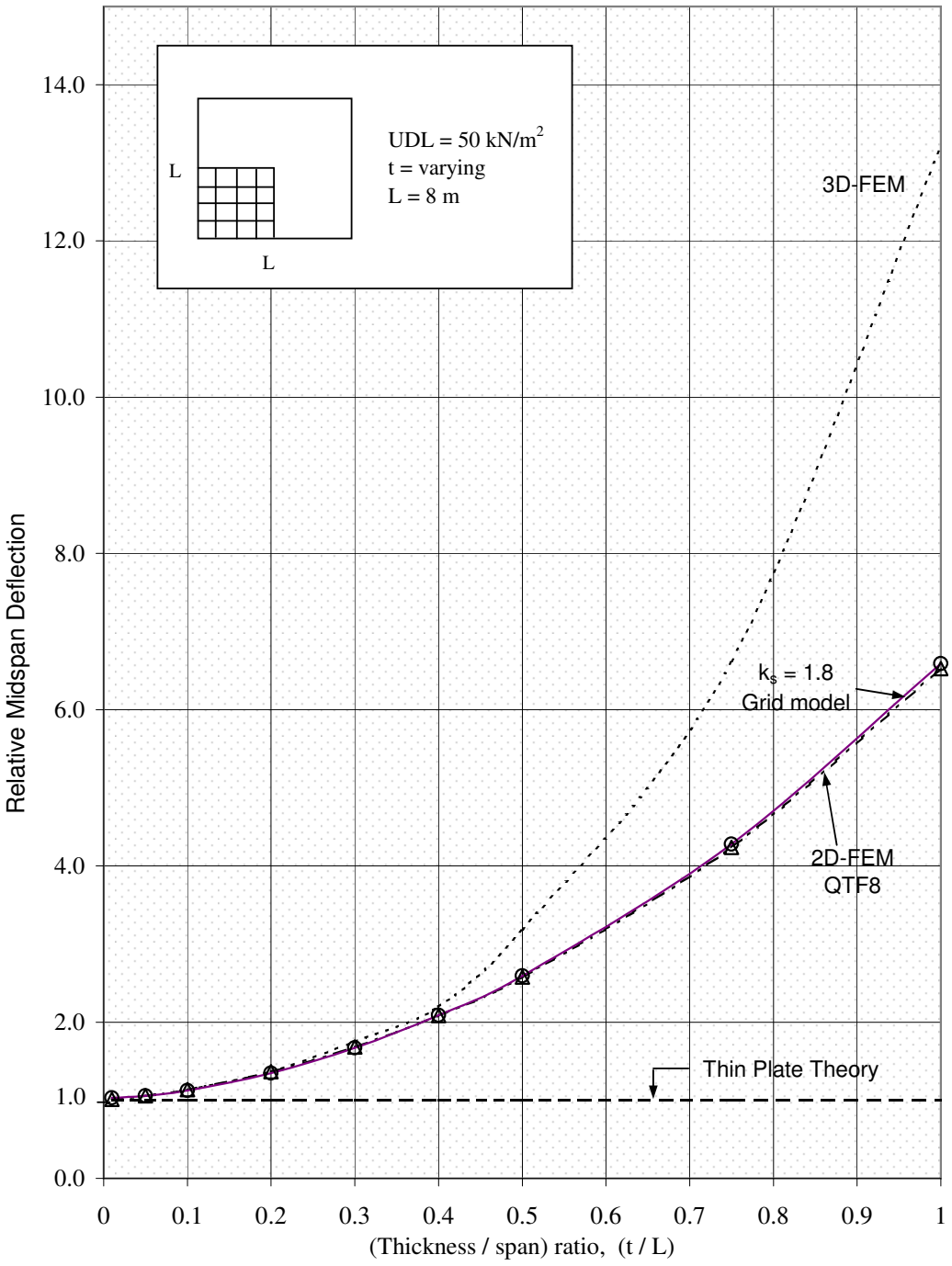

Figure 7.8. Midspan deflections of a square plate for simply supported case - UDL
Thin plate theory deflection is assumed unity

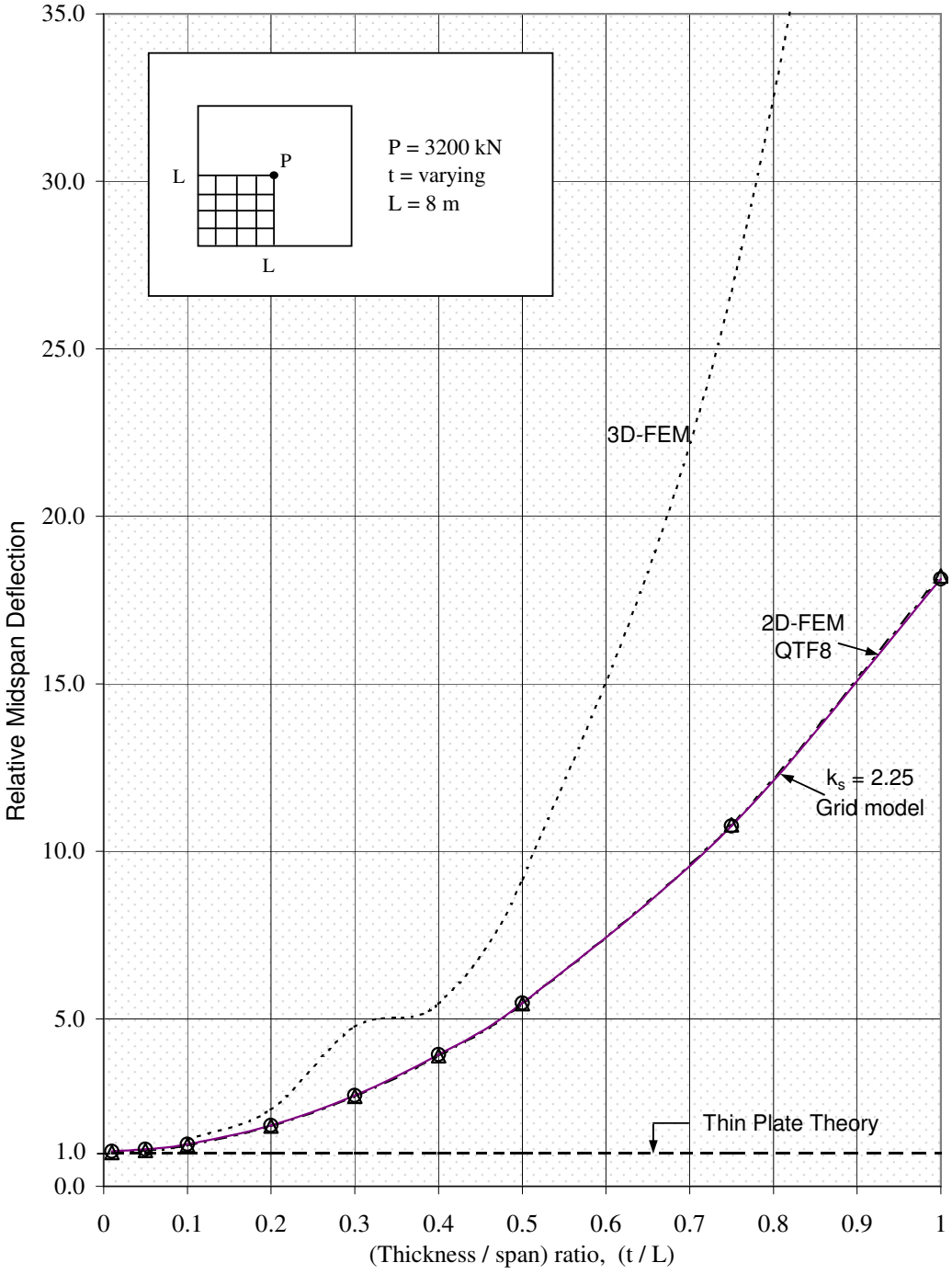

Figure 7.9. Midspan deflections of a square plate for simply supported case -point loading
Thin plate theory deflection is assumed unity

7.2. The Influence of Finer Mesh Size

The square plate model analysed is of a mesh size 4 by 4 which can be classified as coarse mesh size. The plate is also modelled for 10 by 10 elements, medium size, and 16 by 16 elements, fine mesh, for the fixed and simply supported cases and uniformly distributed load. Using the grid framework method with using shape factor k_s = 1.8 for uniformly distributed case, the midspan deflections are calculated and compared with the deflections found by 2D finite elements.

From the Tables 7.7 and 7.8 it can be seen that even with the coarse mesh sufficient accuracy can be obtained. Round of errors that can occur with fine mesh, therefore, medium mesh size (10x10) is (even coarse mesh) is appropriate for the analyses.

Table 7.7. Results for fixed case obtained by finer mesh sizes (normalized by $D / q L^4$) .

t ***(m)***	**t / L**	**2D-FEM**	**Grid Framework**		
			Coarse Mesh ***(4x4)***	**Medium Size Mesh** ***(10x10)***	**Fine Mesh** ***(16x16)***
0.08	0.01	0.001258	0.001290	0.001271	0.001271
0.40	0.05	0.001327	0.001352	0.001331	0.001346
0.80	0.10	0.001505	0.001532	0.001508	0.001522
1.60	0.20	0.002173	0.002203	0.002180	0.002189
2.40	0.30	0.003245	0.003282	0.003261	0.003261
3.20	0.40	0.004730	0.004777	0.004760	0.005174
4.00	0.50	0.006631	0.006690	0.006681	0.006648
6.00	0.75	0.013215	0.013317	0.013333	0.013234
8.00	1.00	0.022424	0.022582	0.022628	0.022445

Table 7.8. Results for simply support case by finer mesh sizes (normalized by $D / q L^4$) .

t *(m)*	t / L	2D-FEM	Grid Framework		
			Coarse Mesh *(4x4)*	Medium Size Mesh *(10x10)*	Fine Mesh *(16x16)*
0.08	0.01	0.004106	0.004187	0.004200	0.004217
0.40	0.05	0.004289	0.004275	0.004334	0.004375
0.80	0.10	0.004617	0.004542	0.004651	0.004695
1.60	0.20	0.005544	0.005415	0.005563	0.005602
2.40	0.30	0.006822	0.006663	0.006838	0.006862
3.20	0.40	0.008457	0.008269	0.008567	0.008490
4.00	0.50	0.010465	0.010227	0.010506	0.010496
6.00	0.75	0.017208	0.016726	0.017318	0.017240
8.00	1.00	0.026490	0.025627	0.026706	0.026541

7.3. Bending Moments

The bending moments obtained from thick plate model and thin plate model are given in Tables 7.9 to 7.11 for uniformly distributed and point loading cases, fixed and simply supported support conditions.

The errors are calculated with taking the difference between the bending moments found from the thin plate model and the bending moments found from the thick plate model. The tables show that with the increasing thickness to span ratio the error in bending moments are increasing. The contours of moment values are given in Figures 7.11 to 7.12 for thickness to span ratio $t/L = 0.4$.

The moment values are plotted in Figures 7.13 to 7.14 for fixed and simply supported cases, uniformly distributed and point loading.

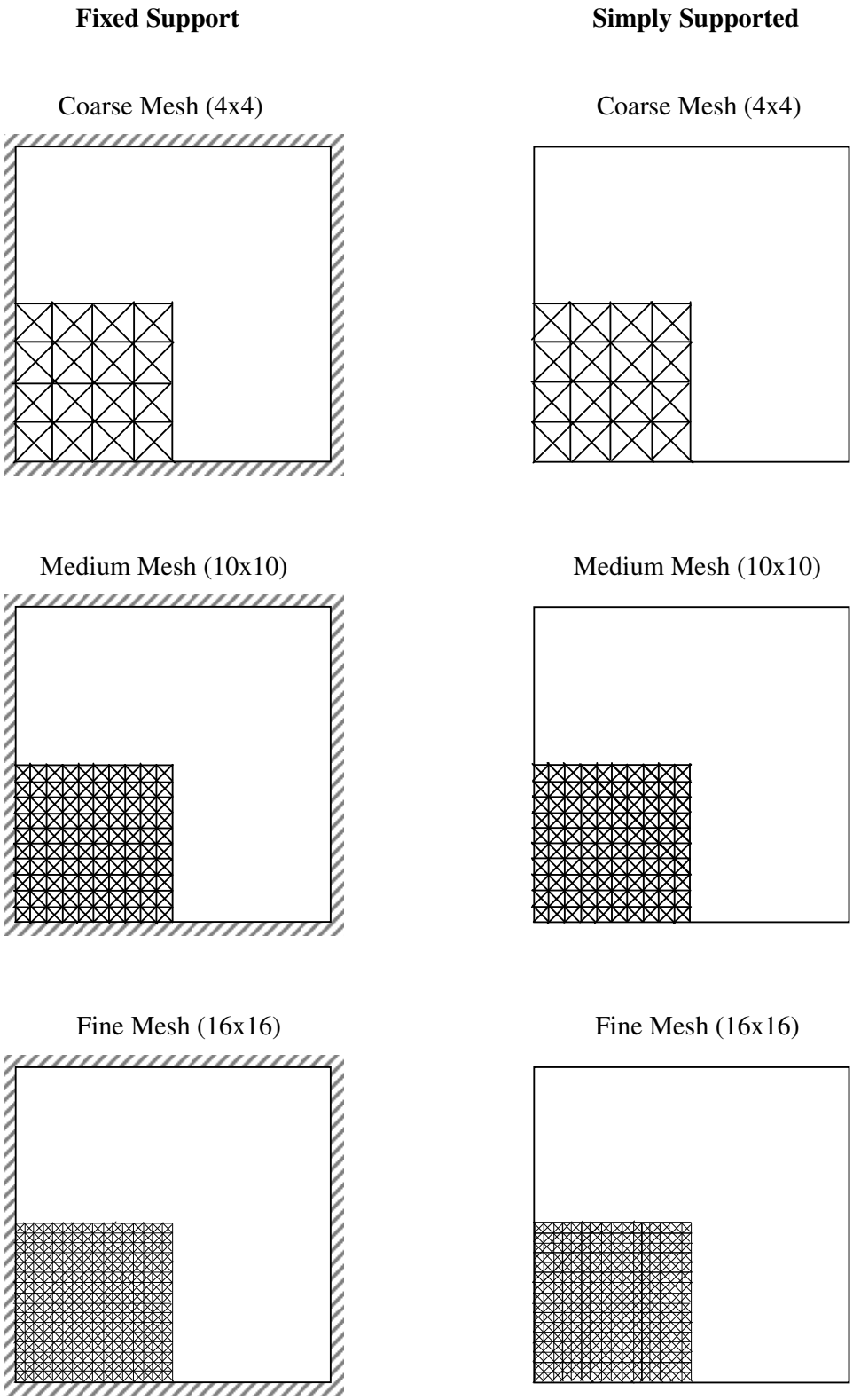

Figure 7.10 Mesh sizes for a quarter square plate

Table 7.9. Bending moments for fixed and uniformly distributed case.

t ***(m)***	**t / L**	**M_x at B** (Mid-side)**,** *kN m*			**M_x at A** (Center)**,** *kN m*		
		Thin Plate	Thick Plate	Error	Thin Plate	Thick Plate	Error
0.08	0.01	160.24	159.40	0.52 %	75.78	75.87	0.12 %
0.40	0.05	160.24	158.67	0.98 %	75.78	76.45	0.88 %
0.80	0.10	160.24	154.83	3.38 %	75.78	77.09	1.73 %
1.60	0.20	160.24	145.40	9.26 %	75.78	78.27	3.29 %
2.40	0.30	160.24	138.98	13.27 %	75.78	78.97	4.21 %
3.20	0.40	160.24	135.29	15.57 %	75.78	79.35	4.71 %
4.00	0.50	160.24	133.13	16.92 %	75.78	79.57	5.00 %
6.00	0.75	160.24	130.61	18.49 %	75.78	79.81	5.32 %
8.00	1.00	160.24	129.62	19.11 %	75.78	79.91	5.35 %

Table 7.10. Bending moments for fixed and point load case.

t ***(m)***	**t / L**	**M_x at B** (Mid-side)**,** *kN m*			**M_x at A** (Center)**,** *kN m*		
		Thin Plate	Thick Plate	Error	Thin Plate	Thick Plate	Error
0.08	0.01	403.08	397.84	1.30 %	1011.9	1018.5	0.65 %
0.40	0.05	403.08	394.53	2.12 %	1011.9	1024.9	1.28 %
0.80	0.10	403.08	379.58	5.83 %	1011.9	1026.9	1.48 %
1.60	0.20	403.08	348.29	13.59 %	1011.9	1030.2	1.81 %
2.40	0.30	403.08	328.57	18.49 %	1011.9	1032.2	2.01 %
3.20	0.40	403.08	317.49	21.23 %	1011.9	1033.2	2.10 %
4.00	0.50	403.08	311.08	22.82 %	1011.9	1033.8	2.16 %
6.00	0.75	403.08	303.64	24.67 %	1011.9	1034.5	2.23 %
8.00	1.00	403.08	300.72	25.39 %	1011.9	1034.8	2.26 %

Table 7.11. Bending moments for simply supported model.

t ***(m)***	**t / L**	**Uniformly Distributed Load** **M_x at A** (Center), *kN m*			**Point Load** **M_x at A** (Center), *kN m*		
		Thin Plate	Thick Plate	Error	Thin Plate	Thick Plate	Error
0.08	0.01	153.21	157.19	2.60 %	1184.4	1193.5	0.77 %
0.40	0.05	153.21	160.98	5.07 %	1184.4	1206.5	1.87 %
0.80	0.10	153.21	165.83	8.24 %	1184.4	1217.2	2.77 %
1.60	0.20	153.21	174.37	13.81 %	1184.4	1235.8	4.34 %
2.40	0.30	153.21	180.84	18.03 %	1184.4	1249.8	5.52 %
3.20	0.40	153.21	185.47	21.06 %	1184.4	1259.7	6.36 %
4.00	0.50	153.21	188.74	23.19 %	1184.4	1266.7	6.95 %
6.00	0.75	153.21	193.37	26.21 %	1184.4	1276.5	7.78 %
8.00	1.00	153.21	195.55	27.64 %	1184.4	1281.1	8.16 %

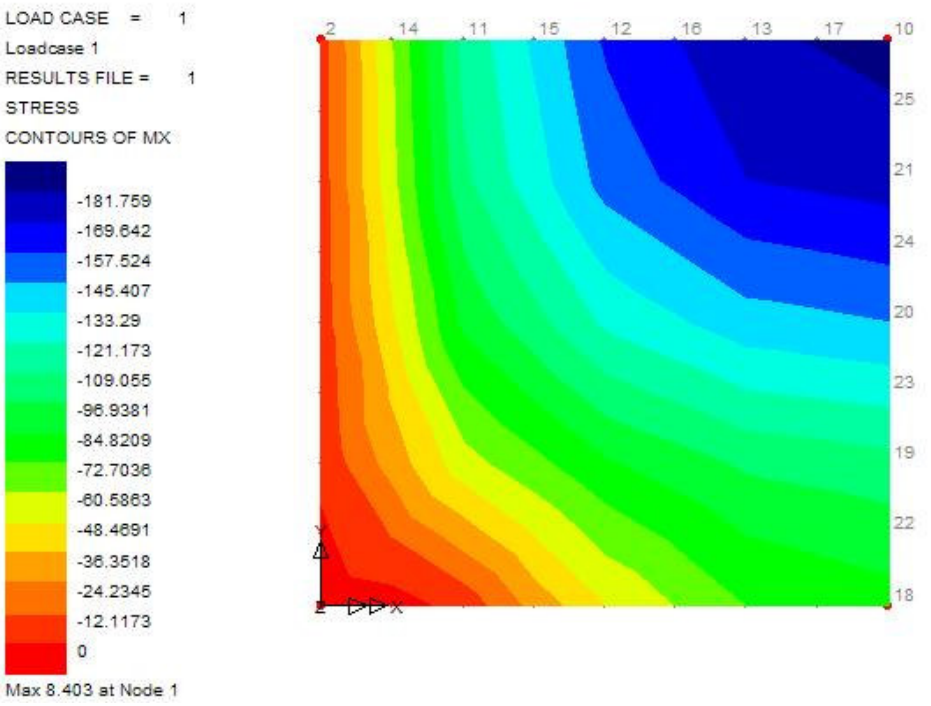

Figure 7.11 Bending moment contours for thick plate, simply supported case and UDL (t/L=0.4)

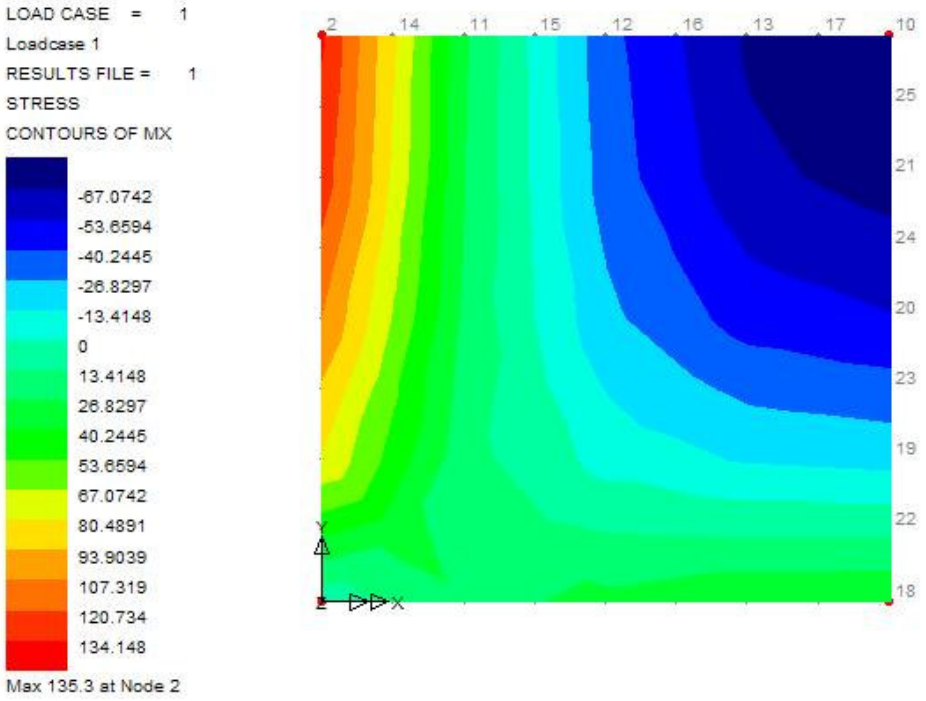

Figure 7.12 Bending moment contours (M_x) for thick plate, fixed case and UDL (t/L=0.4)

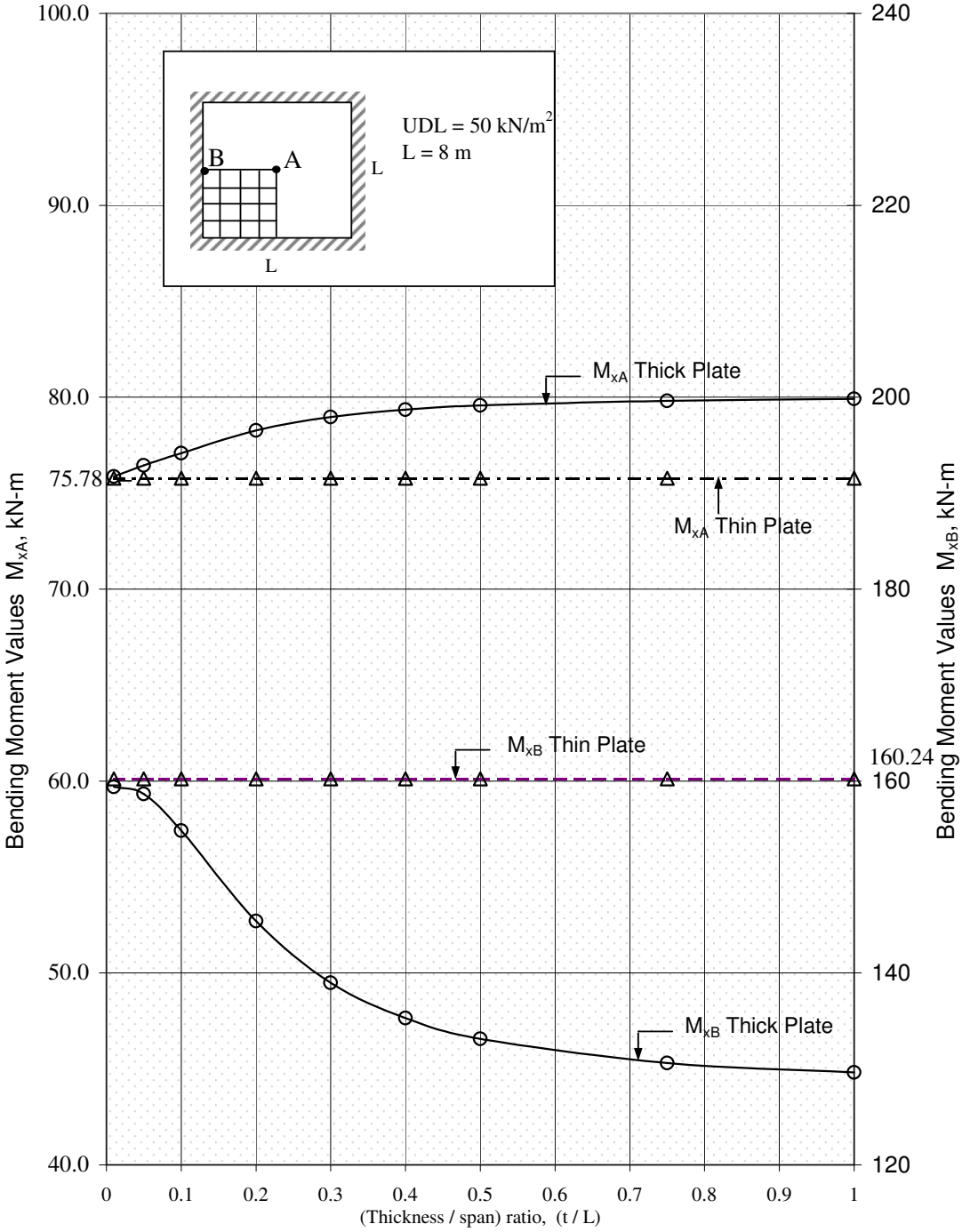

Figure 7.13. Bending moments of a square plate for fixed case - UDL

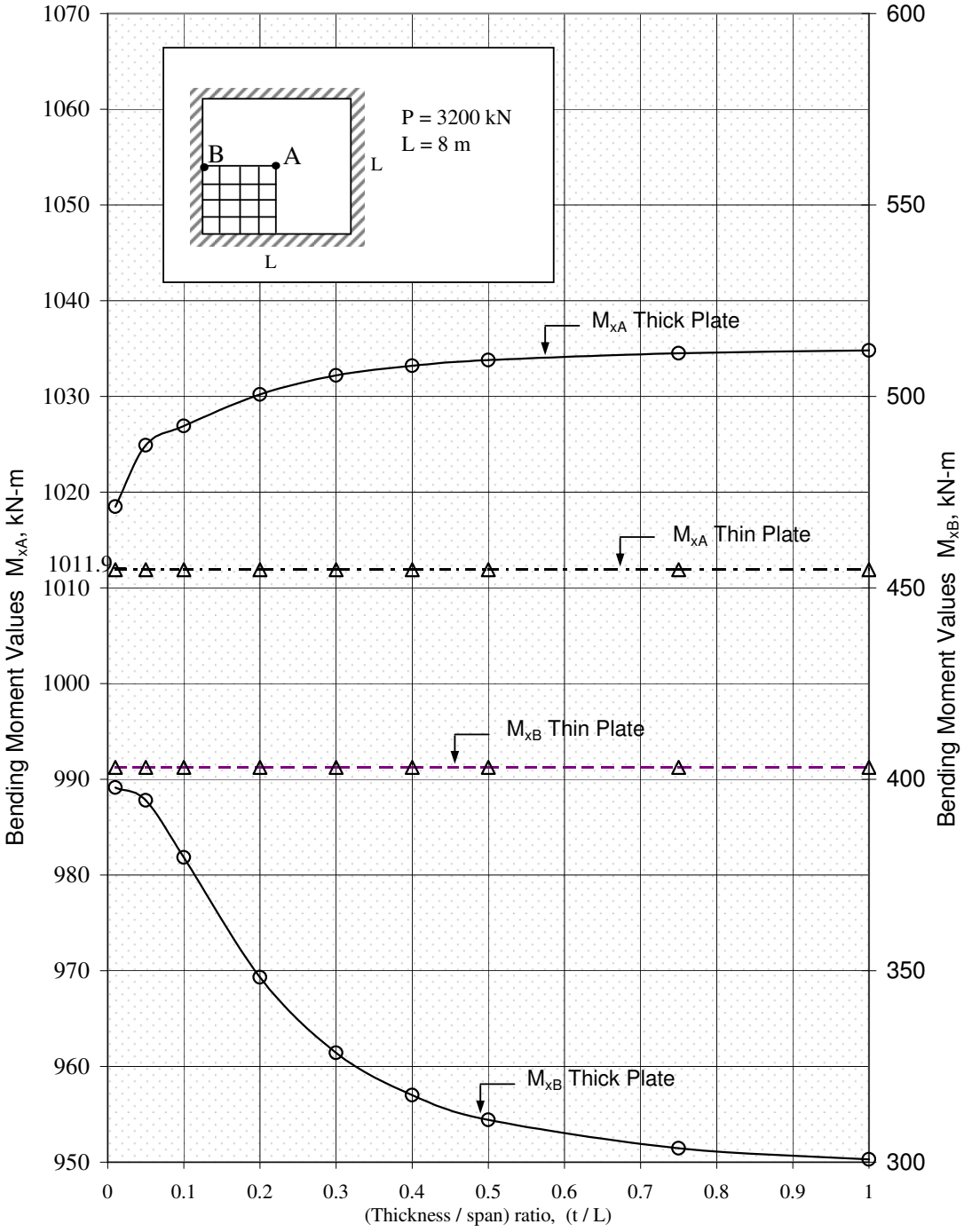

Figure 7.14. Bending moments of a square plate for fixed case - Point loading

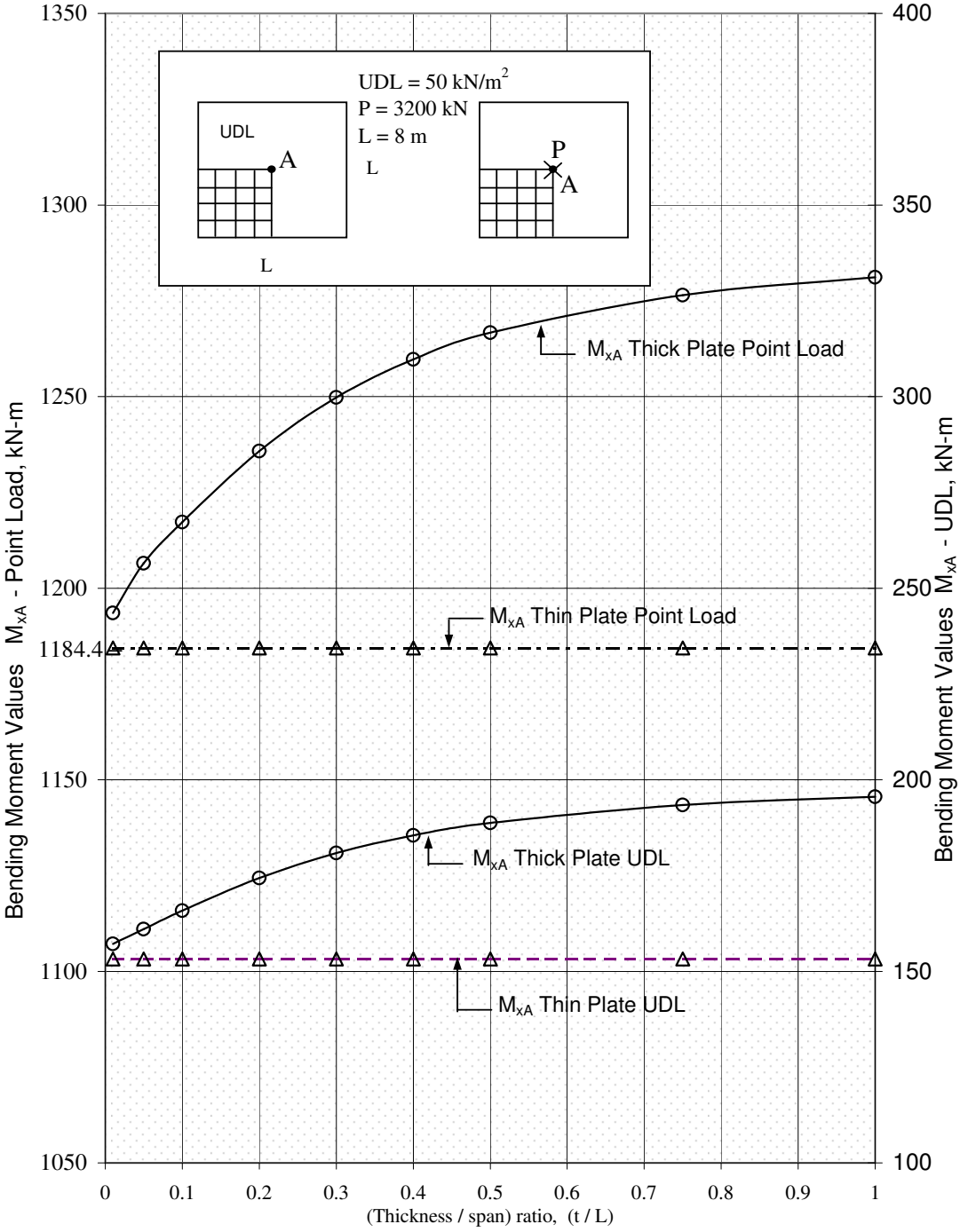

Figure 7.15. Bending moments of a square plate for simply supported case

7.4. Rectangular Plate Model

The grid framework method is also checked by a rectangular plate of size 6 x 10 m and with a 4 by 4 mesh size for fixed and simple support cases and uniformly distributed and point loads. The loading is taken as q = 50 kN/m^2 as uniformly distributed load and P = 3000 kN as point load. Again the shape factor for UDL is k_s = 1.8 and for point load case k_s = 2.25.

In the Figure 7.16 the uniformly distributed case results are plotted with ratios of results obtained from thin plate theory. It can be seen from the figure that the results of grid framework method where shear deformations are taken into account, defined herein, are matching with 2D-FEM element for thick plate. And in Figure 7.17 the results of point loading case are plotted, where shape factor is k_s = 2.25 for point loading case. The results give sufficient accuracy also for point loading case with k_s = 2.25.

Table 7.12. Midspan deflection of rectangular plate with UDL (w = r D / q L^4).

t ***(m)***	**t / L**	**Fixed**			**Simply supported**		
		Thin Plate 2D-FEM	Thick Plate 2D-FEM	Grid Work	Thin Plate 2D-FEM	Thick Plate 2D-FEM	Grid Work
0.06	0.01	0.001763	0.001759	0.001789	0.006356	0.006548	0.06732
0.30	0.05	0.001763	0.001833	0.001860	0.006356	0.006726	0.06792
0.60	0.10	0.001763	0.002025	0.002129	0.006356	0.007067	0.07273
1.20	0.20	0.001763	0.002768	0.002818	0.006357	0.008055	0.08038
1.80	0.30	0.001763	0.003965	0.004024	0.006355	0.009457	0.009441
2.40	0.40	0.001763	0.005604	0.005675	0.006356	0.011270	0.011279
3.00	0.50	0.001763	0.007551	0.007772	0.006353	0.013504	0.013547
4.50	0.75	0.001763	0.014858	0.014963	0.006357	0.020958	0.021102
6.00	1.00	0.001763	0.024849	0.025034	0.006356	0.031154	0.031394

Table 7.13. Midspan deflection of rectangular plate with Point Load ($w = r\ D / P\ L^2$).

T ***(m)***	**t / L**	**Fixed**			**Simply supported**		
		Thin Plate 2D-FEM	Thick Plate 2D-FEM	Grid Work	Thin Plate 2D-FEM	Thick Plate 2D-FEM	Grid Work
0.06	0.01	0.008877	0.008819	0.009063	0.019818	0.019900	0.020883
0.30	0.05	0.008877	0.009547	0.09718	0.019815	0.020810	0.021609
0.60	0.10	0.008877	0.011470	0.011628	0.019821	0.023008	0.023661
1.20	0.20	0.008879	0.019033	0.018923	0.019819	0.031005	0.031319
1.80	0.30	0.008877	0.031451	0.030783	0.019823	0.038201	0.043578
2.40	0.40	0.008879	0.048703	0.047209	0.019810	0.061319	0.060352
3.00	0.50	0.008877	0.070759	0.068140	0.019815	0.083620	0.081696
4.50	0.75	0.008878	0.147019	0.140586	0.019819	0.160521	0.154900
6.00	1.00	0.008880	0.253571	0.241758	0.019821	0.267445	0.256662

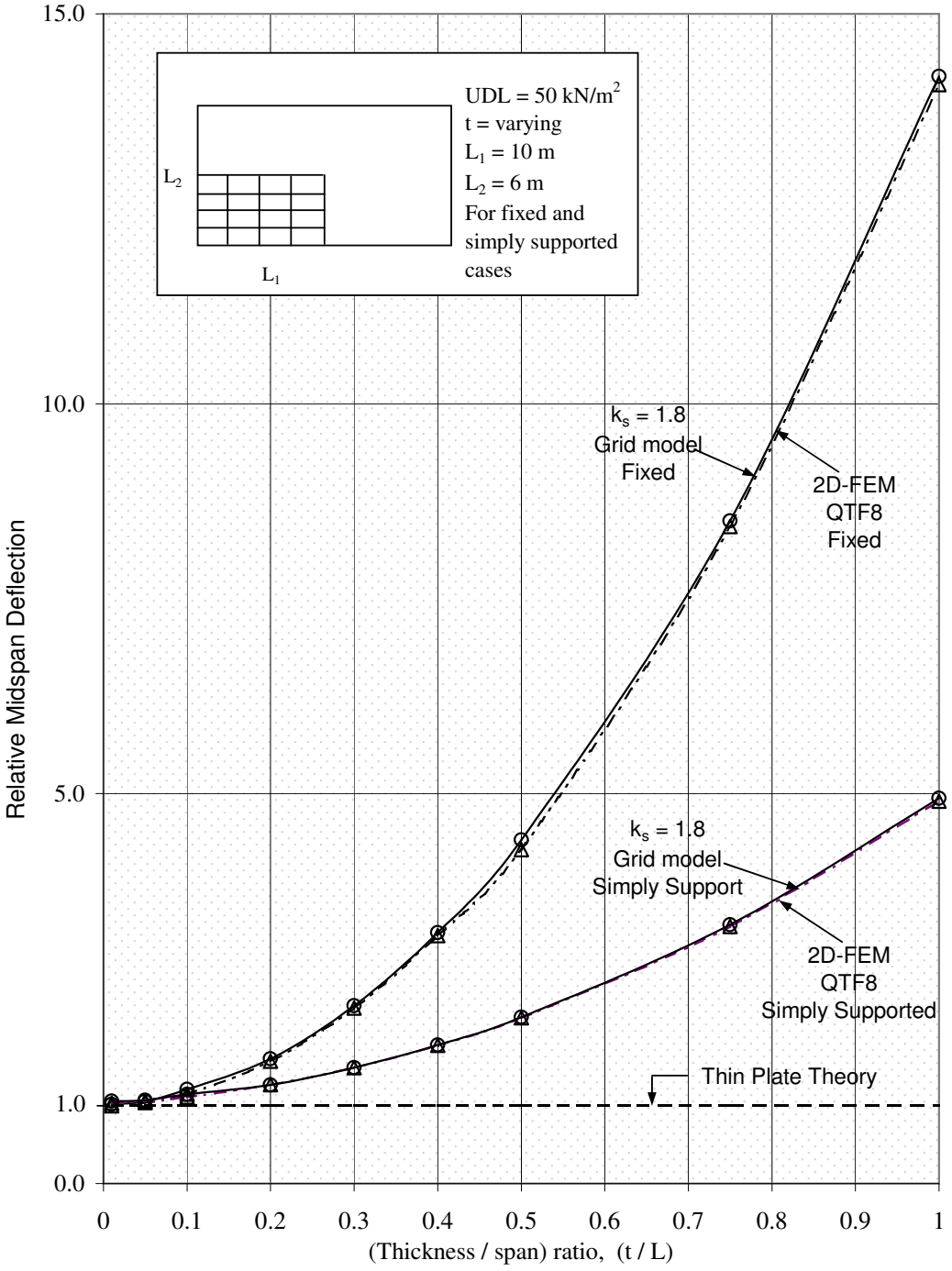

Figure 7.16. Midspan deflections of a rectangular plate for uniformly distributed case
Thin plate theory deflection is assumed unity

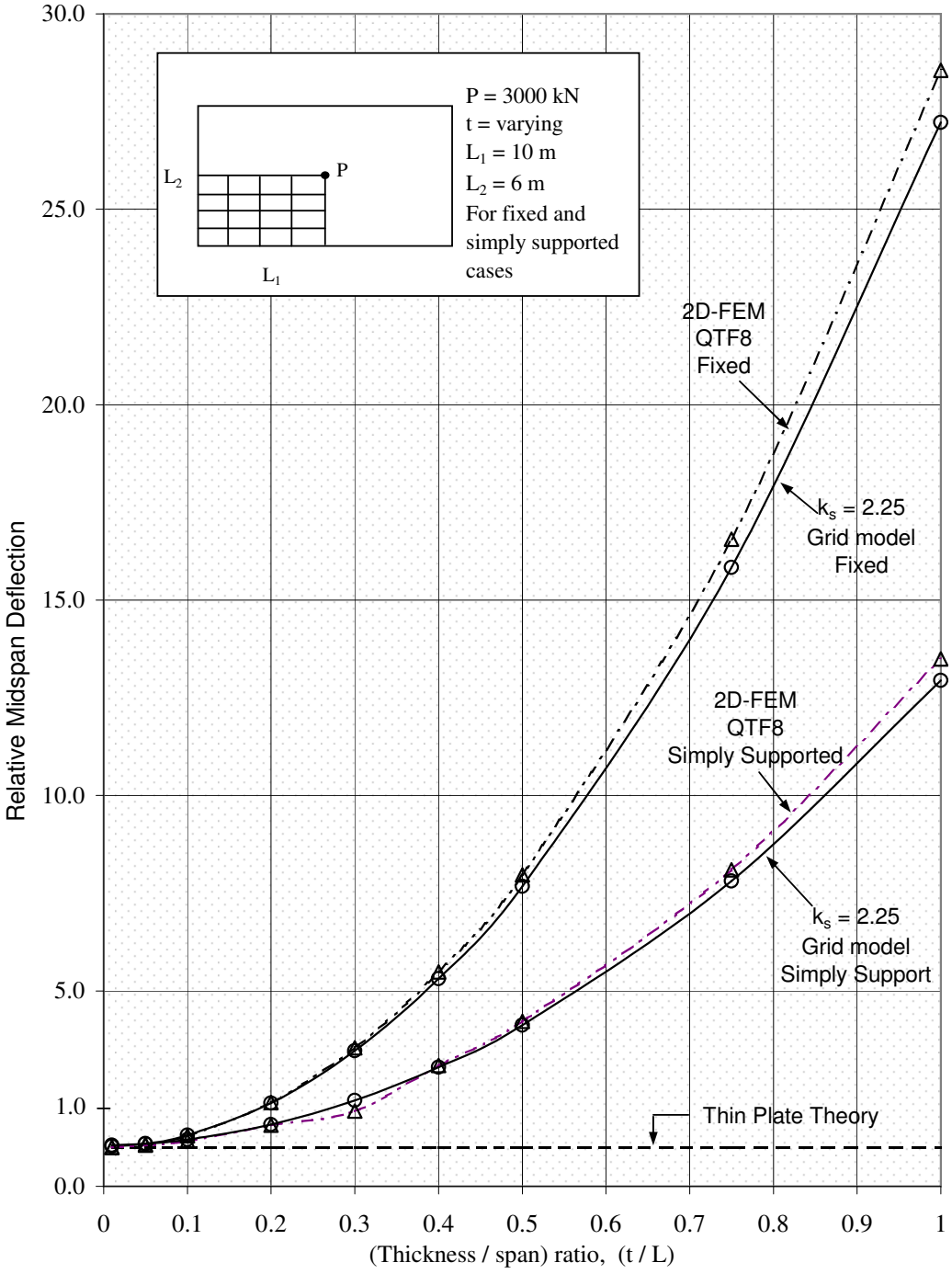

Figure 7.17. Midspan deflections of a rectangular plate for point loading case
Thin plate theory deflection is assumed unity

7.5. Foundation Analysis of 53rd at Third Building with Grid Framework Method

The office building located at 53rd and Third Avenue in New York, USA, has an elliptical floor plan and 39 storey height as shown in Figure 7.18. The foundation of this building is analysed to illustrate how easily the grid framework method can be applied to real problems.

The foundation of the building is also elliptical in shape and four meters thick. The floor plan is given in Figure 7.19. The foundation is modelled with grid framework using 0.5 m wide elements. Again one quarter of the foundation is modelled due to two-way symmetry (Figure 7.20).

The load at each floor is taken as $q = 15$ kN/m^2, therefore, totalling $q = 585$ kN/m^2 at foundation level acting from bottom to top. The foundation is 60 m long in x-direction and 30 m wide in y-direction, therefore, the foundation model is divided into 60 x 30 elements. The nodes and the columns are shown in Figure 7.17.

The analysis is conducted with the framework method by taking into the shear deformations where the shape factor $k_s = 1.8$ since the loading is uniformly distributed load. The same model is also analysed with thin plate elements to illustrate the error introduced.

After the analysis the maximum deflection is found to be 2.015 mm for thick plate analysis. When the same model is used for thin plate analysis where the shear deformations are neglected, the maximum deformation is calculated as 0.896 mm.

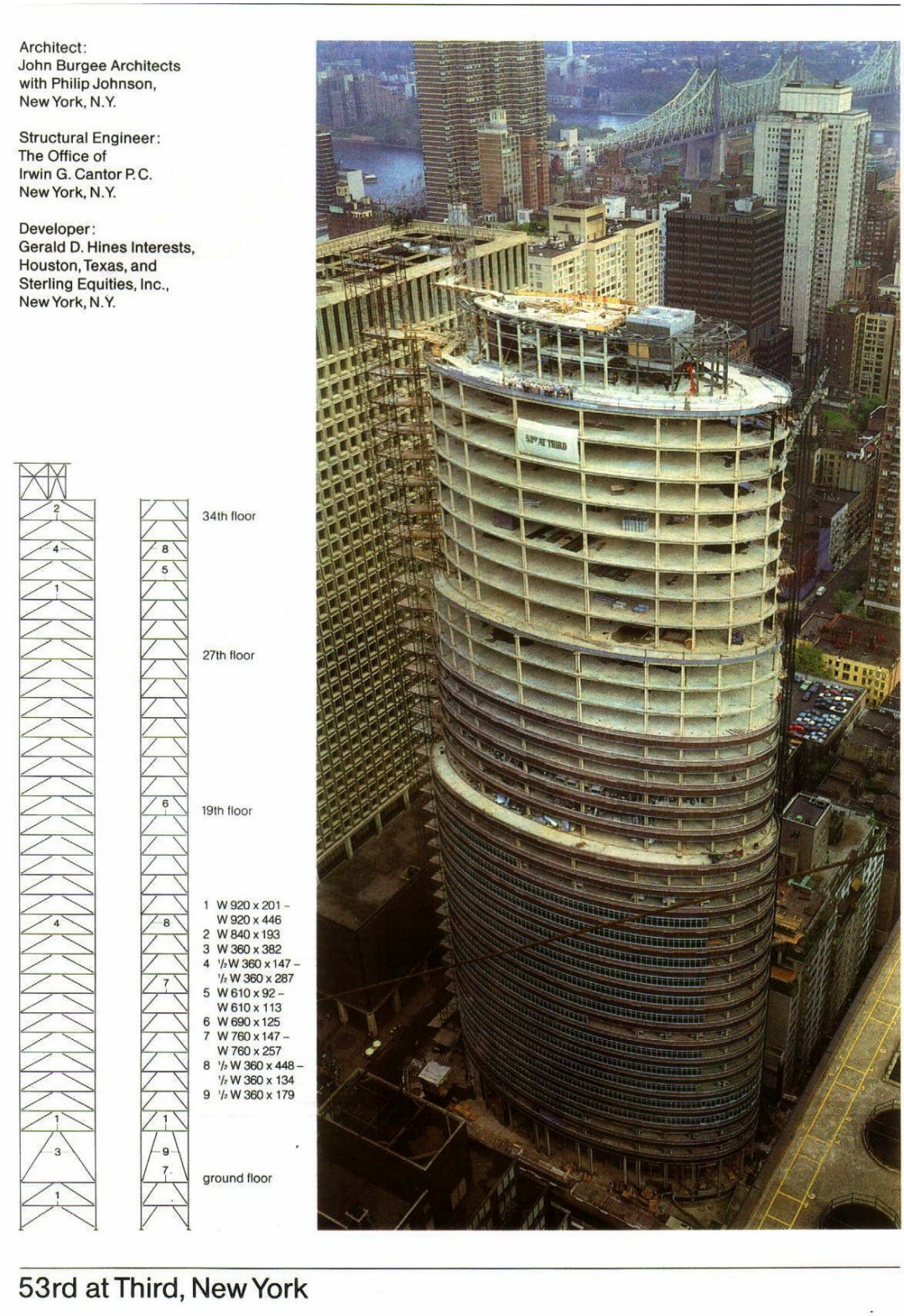

Figure 7.18. The 53rd at Third building in New York

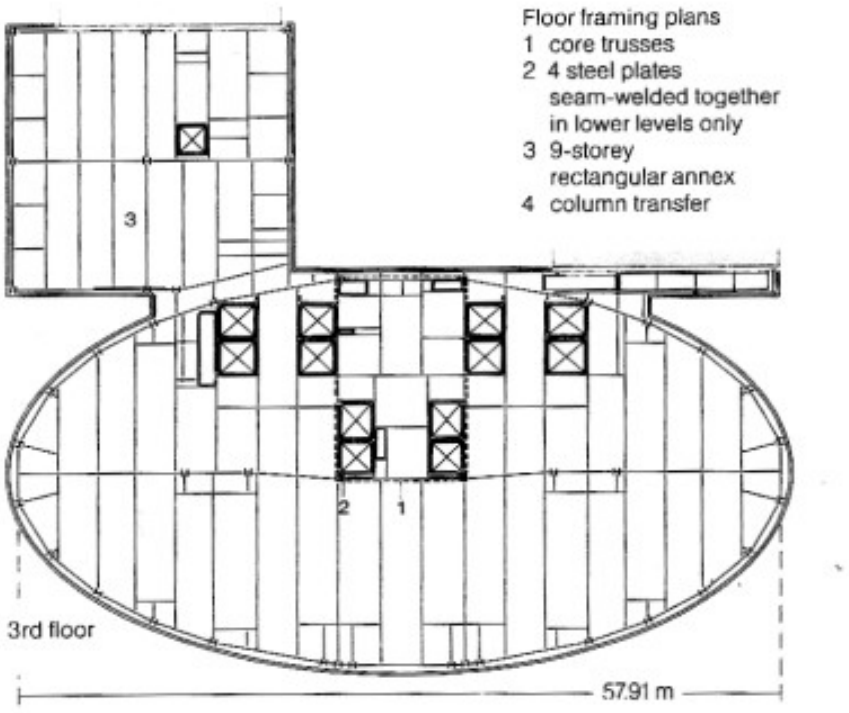

Figure 7.19. The floor plan of 53rd at Third building.

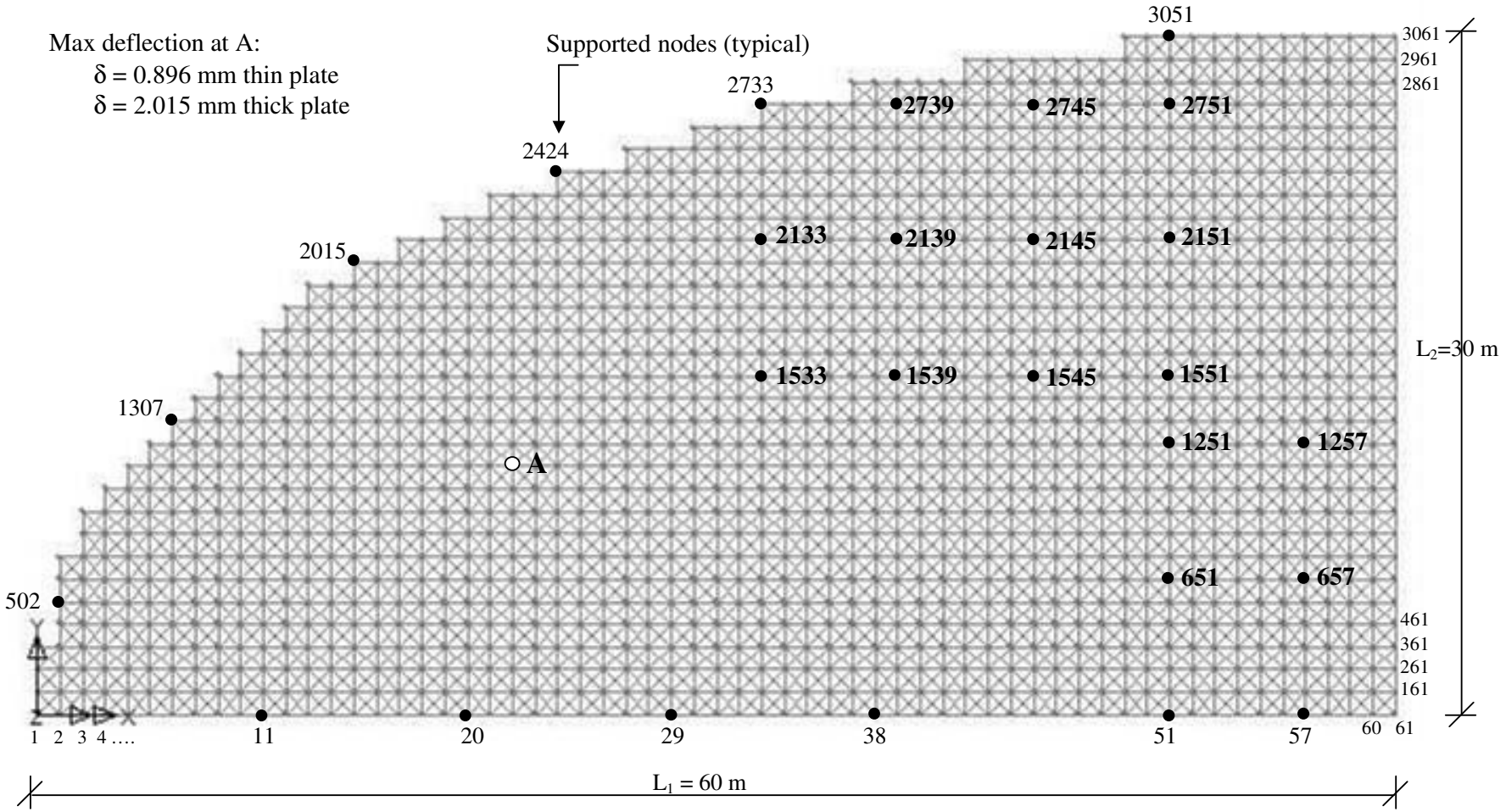

Figure 7.20. The foundation model with grid framework method
(Skyscaper 53rd at Third, New York, USA)

8. CONCLUSIONS

In this Thesis the shear deformation theory in thick plate bending problems is studied with 2D continuum elements and also an alternative method using grid framework models is presented. Based on the studies contained herein some concluding remarks may be stated as follows:

1) The errors in deformations become significant when thickness to span ratio of plates is greater than 0.1. The error for instance, may be as high as 375 per cent when the thickness to span ratio is 0.4. Therefore, it is almost compulsory to consider the thick plate theory and consequently the shear deformations when the thickness to span ratio of a plate exceeds 0.1.

2) When plates are formulated in accordance with the shear deformation theory of Mindlin, the finite elements with three degrees of freedom at each node require extensive amounts of formulations to be handled when compared with the classical thin plate theory. This is very time consuming especially when large systems are to be solved. However, the specially developed grid framework method introduced herein is easily programmable and the computation time is relatively very short.

3) It is seen in the illustrative examples that, with the application of appropriate shear correction factors, the grid framework method produces very accurate results, even for very thick plates.

4) The special 1D grid framework technique is very easy to program when compared with continuous finite elements. The theory used in considering the influence of shear deformations is not as complicated as the sophisticated solid finite elements of Mindlin theory. Further, the execution time is considerably less, because the entire thick plate theory is represented by means of very simple looking shear correction factors.

REFERENCES

1. Hrennikoff, A. “Solutions of problems of elasticity by the framework method” *Journal of Applied Mechanics*, Vol 63, New York, December 1941.

2. Todhunter, J. And K. Pearson. *History of the Theory of the Elasticity,* Vol. 1 New York, Dover Publications Inc.

3. Poisson, G.D., *Memoire sur L’Equiblibre et le Measurement des Corps Solide*, Memoirs of the Academy, Vol. 8, Paris, 1829.

4. Kirchhoff, G., Vorlesungen Uber Mathematische Physik, Vol. I. *Mechanic:* 1876.

5. Newmark, N.M., “Numerical Methods of Analysis of bars, plates, and Elastic bodies.” *Numerical Methods of Analysis in Engineering. Ed L. E Grinter. New York*: The MacMillan Co., 1949.

6. Ang., A.H.S., and N.M. Newmark. “A Numerical Procedure for the Analysis of the continuous plates” *Proceedings, 2nd ASCE Conference on Electronic Computation*, Pitssburgh, 1960.

7. Yettram, S.L. and H.M. Husain. “Grid-Framework Method for plates in Flexure.” *Journal of the Engineering Mechanics Division*, Asce, Vol.91. New York : June, 1965.

8. Christensen, R.M. “Vibration of a Right Triangular Cantilever Plate by a Gridwork Method” *Journal American Ins. Of Aeronautics and Astronautics*, Vol.1 (1964), 1790-1795.

9. Lightfoot, E. “A grid Framework Analogy for Laterally Loaded Plates” *International Journal of Mechanical Sciences*, Vol. 6. Oxford: Pergamon Pres, June, 1964.

10. Turner, M.J., R.W. Clough, H.C. Martin and L.J. TOPP, "Stiffness and Deflection Analysis of Complex Structures"*, J. Aero Sci*., 23 No:9, 805-823 (1956).

11. Adini, A. and R.W. Clough, "Analysis of Plate Bending by the Finite element method", *Report to the National Science Foundation*, Grant G 7337 (1961).

12. Melosh, R.J., "A Stiffness Matrix for the Analysis of Thin Plates in Bending", *J. Aero, Science*, 28, 34 (1961).

13. Melosh, R.J., "Basis for derivation of Matrices for the Direct Stiffness Method", *AIAA Journal*, 1, 1631-1637 (1963).

14. Clough, R.W. and J.L. Tocher, "Finite Element Stiffness Matrices for the analysis of plate bending", *Proc. Conf. ,on Matrix Methods in Structural Mechanics*, Wright-Patterson AFB Ohio (1965).

15. Zienkiewicz, O.C. and Y.K. Cheung, *The Finite Element Method in Structural and Continuum Mechanics Mechanics*, McGraw-Hill Ltd. London (1967).

16. Melosh, R.J., *Structural Analysis of Solids*, Proc. Amer. Soc. Civ. Eng., ST4, 205-23 (1963).

17. Argyris, J.H. "Continua and Discontinua" *Proc. Conf. Matrix Methods in structural mechanics*, Wright Patterson Air Force Base, Ohio, Oct. (1965).

18. Fjeld, S., *Three Dimensional Theory of Elastics, Finite Element Methods in stress analysis*, ed. I. Holand and K. Bell., Tech. Univ. Of Norway Tapir Press, Trondheim (1969).

19. Reissner, E. (1947). "On bending of elastic plates." *Quarterly of Applied Mathematics*, Vol 5 No:1, pp.55-68.

20. Mindlin, R.D. (1951). "Influence of Rotatory Inertia and Shear on Flexural Motions of Isotropic, Elastic Plates" *Journal of Applied Mechanics*, Vol.18, No.1, pp. 31-38.

21. Utku, Ş., "Stiffness Matrices for Thin Triangular Elements of Nonzero Gaussian Curvature", *AIAA Journal* 5, No. 9 1659-1667.

22. Ray, W. Clough and Felippa, Carlos A., "A refined Quadrilateral element for analysis of Plate Bending", *Proc. Conf, on matrix methods in Structural Mechanics*, Wright-Patterson AFB 1968, AFFOL –TR-68-150, 399-441 (1968).

23. Timoshenko, S. and S. Woinowsky-Krieger, *Theory of Plates and Shells*, Mc-Graw Hill, New York, 1959

24. Wang, C.M., J.N. Reddy, and K.H. Lee, *Shear Deformable Beams and Plates*, Elsevier, 2000

25. Reissner, E., "The effect of transverse shear deformation on bending of elastic plates", *J. Appl. Mech.*, Vol. 12, pp.69-76, (1945).

26. Wittrick, W.H., "Analytical, three-dimensional elasticity solutions to some plate problems, and some observations on Mindlin's plate theory", *Int. J. Solids and Structures,* Vol. 23, pp. 441-464, (1987).

27. Logan, D.L., *A First Course in The Finite Element Method*, Brooks / Cole Thomson Learning, 2002

28. Özdemir, Y.I. and Y. Ayvaz, "Analysis of Clamped and Simply Supported Thick Plates Using Finite Element Method", Sixth *International Congress on Advances in Civil Engineering*, Boğaziçi University, Istanbul, Turkey, 6-8 October 2004

29. Lucas, W.M., "Analysis of Plates with Free Edges on Elastic Winkler Foundations by the Grid Framework Method, *PhD Thesis, Oklahoma University*, 1970

30. Tezcan, S.S., "Computer Analysis of Plane and Space Structures", *Journal of the Structural Division, Proceedings of ASCE*, Vol. 92, No. ST2, Paper No. 4780, pp. 143-173, April 1966.

31. Tezcan, S.S., "A Rectangular Finite Element for Analysis of Thick Plate Bending", *Bull. Tech. Univ. Istanbul*, Vol. 41, pp. 315-331, 1988.

32. *LUSAS Finite Element System*, Version 13.5. *LUSAS Theory Manual 2*, FEA Ltd., Surrey, England

33. *LUSAS Finite Element System*, Version 13.5. *LUSAS Element Library*, FEA Ltd., Surrey, England